Stem Cell Reports
Article

ISSCR

OPEN ACCESS

Human Intestinal Tissue with Adult Stem Cell Properties Derived from Pluripotent Stem Cells

Ryan Forster,[1] Kunitoshi Chiba,[1] Lorian Schaeffer,[1] Samuel G. Regalado,[1] Christine S. Lai,[2] Qing Gao,[2] Samira Kiani,[2] Henner F. Farin,[3] Hans Clevers,[3,4] Gregory J. Cost,[5] Andy Chan,[5] Edward J. Rebar,[5] Fyodor D. Urnov,[5] Philip D. Gregory,[5] Lior Pachter,[1,6] Rudolf Jaenisch,[2,4,7,*] and Dirk Hockemeyer[1,*]

[1]Department of Molecular and Cell Biology, University of California, Berkeley, Berkeley, CA 94720-3370, USA
[2]The Whitehead Institute for Biomedical Research, Cambridge, MA 02142, USA
[3]Hubrecht Institute, Royal Netherlands Academy of Arts and Sciences, University Medical Center Utrecht, 3584 Utrecht, the Netherlands
[4]Skolkovo Institute of Science and Technology (Skoltech), Novaya str. 100, Skolkovo, Moscow Region 143025, Russia
[5]Sangamo BioSciences, Richmond, CA 94804, USA
[6]Department of Mathematics and Computer Science, University of California, Berkeley, Berkeley, CA 94720-3840, USA
[7]Department of Biology, Massachusetts Institute of Technology, Cambridge, MA 02139, USA
*Correspondence: jaenisch@wi.mit.edu (R.J.), hockemeyer@berkeley.edu (D.H.)
http://dx.doi.org/10.1016/j.stemcr.2014.05.001

SUMMARY

Genetically engineered human pluripotent stem cells (hPSCs) have been proposed as a source for transplantation therapies and are rapidly becoming valuable tools for human disease modeling. However, many applications are limited due to the lack of robust differentiation paradigms that allow for the isolation of defined functional tissues. Here, using an endogenous LGR5-GFP reporter, we derived adult stem cells from hPSCs that gave rise to functional human intestinal tissue comprising all major cell types of the intestine. Histological and functional analyses revealed that such human organoid cultures could be derived with high purity and with a composition and morphology similar to those of cultures obtained from human biopsies. Importantly, hPSC-derived organoids responded to the canonical signaling pathways that control self-renewal and differentiation in the adult human intestinal stem cell compartment. This adult stem cell system provides a platform for studying human intestinal disease in vitro using genetically engineered hPSCs.

INTRODUCTION

Human embryonic stem cells (hESCs) and induced pluripotent stem cells (hiPSCs) (Takahashi et al., 2007), collectively referred to as human pluripotent stem cells (hPSCs), are currently used in disease modeling to address questions specific to humans and to complement insights gained from other model organisms (Soldner and Jaenisch, 2012; Soldner et al., 2011). Genetic engineering using site-specific nucleases was recently established in hPSCs (Dekelver et al., 2010; Hockemeyer et al., 2009, 2011; Yusa et al., 2011; Zou et al., 2009), allowing a level of genetic control that was previously limited to model systems. We can now target gene knockouts, generate tissue-specific cell lineage reporters, overexpress genes from a defined locus, and introduce or repair single-point mutations in hPSCs. Realizing the full potential of hPSCs will require robust differentiation protocols. Most current protocols isolate individual cell types rather than establish functional tissues. Although the former methods can identify cell-autonomous phenotypes, the study of cell-nonautonomous disease mechanisms necessitates a defined tissue context in which individual cell types are represented with the same stoichiometry and architecture as occur in vivo. The recent establishment of human intestinal tissue as in vitro organoid cultures from hPSCs and primary tissue represents a major advance toward creating such a model system for human tissue (Jung et al., 2011; McCracken et al., 2011; Ootani et al., 2009; Sato et al., 2009, 2011b; Spence et al., 2011). Intestinal organoid cultures comprise tissue-specific differentiated cell types and adult stem-like progenitor cells that self-renew and differentiate, by growth factor induction, into the respective cell types of the intestinal epithelium. Here, we establish a protocol that can enrich for intestinal cells with adult stem character. We first generated an hESC line using gene editing that specifically labeled intestinal adult stem cells using a fluorescent reporter placed into an endogenous gene, and then used this cell line to identify and isolate adult stem cells from a pool of heterogeneous cell types during the differentiation of hPSCs.

We focused on a member of the leucine-rich repeat-containing G protein-coupled receptor (LGR) protein class, LGR5 (McDonald et al., 1998). LGR5 functions within the Wingless-related integration site (WNT) signaling cascade, which maintains the adult intestinal stem cell compartment (de Lau et al., 2011). LGR5 is activated by its ligand, R-spondin (RSPO1) (Carmon et al., 2011; de Lau et al., 2011; Kim et al., 2005; Ruffner et al., 2012), and has been shown by genetic lineage tracing experiments to mark intestinal stem cells (Barker et al., 2007). LGR5-expressing cells at the base of the intestinal crypt

exhibit WNT-dependent self-renewal and can differentiate into all cell types of the adult intestine (Snippert et al., 2010). Together, LGR5-expressing cells and Paneth cells form the adult stem cell niche and are sufficient to establish in vitro organoid cultures from mice (Sato et al., 2011b). Such murine in vitro organoids can be maintained over time in 3D Matrigel cultures under defined conditions that support either WNT-dependent self-renewal of adult stem cells or differentiation by the withdrawal of WNT and Notch signaling (Korinek et al., 1998; Pellegrinet et al., 2011; van Es et al., 2005). Similarly, human organoid cultures lacking stromal components can be derived from primary tissue biopsies when supplemented with additional small-molecule signals (Jung et al., 2011; Sato et al., 2009, 2011a), and in vitro hPSC-derived organoids can be maintained under a variety of conditions (Jung et al., 2011; McCracken et al., 2011; Sato et al., 2011a; Spence et al., 2011; Wang et al., 2013) and used in human disease modeling (Dekkers et al., 2013). Importantly, LGR5-positive mouse colon cells can form organoids that can be expanded ex vivo and allogenically transplanted into colitis models (Fordham et al., 2013; Yui et al., 2012), suggesting that human intestinal tissue might be amenable to transplantation therapies.

Here, we report tools that allow for the isolation of adult intestinal stem cells and intestinal organoid cultures from direct differentiation of hPSCs using standard teratoma differentiation assays. Cultures with posterior gut qualities and expression profiles closely resembling those of human intestinal tissue can be derived and progressively enriched. Our strategy is based on direct isolation of LGR5-positive intestinal cells, a cell type that is only acquired over extended periods by other protocols (Cao et al., 2011; McCracken et al., 2011; Ogaki et al., 2013; Spence et al., 2011; Wang et al., 2011). Functional analysis and mRNA expression profiling of these organoid cultures confirmed the presence of a subset of adult stem cells. We expect that genetically engineering the parent hPSCs of an in vitro human intestinal tissue will provide a model for investigating human intestinal pathophysiology.

RESULTS

Genome Editing the Endogenous Human LGR5 Locus in hPSCs to Isolate Adult Intestinal Stem Cells

Based on previous studies that used LGR5 expression to identify (Barker et al., 2007) and isolate (Sato et al., 2011b) adult intestinal stem cells in mice, we tested whether a similar approach could be used to isolate and characterize gastrointestinal tissue derived from hPSCs. We developed two Zinc Finger Nuclease (ZFN) pairs that target the LGR5 gene in either the first (LGR5-GFP$^{N\text{-term}}$) or last coding exon (LGR5-GFP$^{C\text{-term}}$; Figure 1A; Figure S1A available online). We coelectroporated these ZFNs and their corresponding donor plasmids into WIBR3 hESCs (Lengner et al., 2010) to integrate a GFP cassette together with a PGK-Puromycin into the LGR5 locus (Figure 1A). Southern blot analysis using external and internal probes (Figures S1A and S1B) and sequence analysis in subsequent RNA sequencing (RNA-seq) confirmed the correct junction of the LGR5 gene with the GFP reading frame at either position. The targeting efficiencies for the generation of LGR5-GFP$^{N\text{-term}}$ and LGR5-GFP$^{C\text{-term}}$ cell lines were 18.75% and 6.25%, respectively.

Initially, we characterized this new LGR5 reporter system using a previously established protocol for the direct differentiation of hPSCs to intestinal cells (McCracken et al., 2011; Spence et al., 2011; data not shown). In order to enrich more of the later steps of differentiation with increased LGR5 expression, we capitalized on our previous observation that in teratoma formation assays, some regions of the teratoma differentiate into intestinal-like tissues (Figures 1B, S1C, and S2D). When we performed these teratoma formation assays with the LGR5-GFP reporter cells, we were able to specifically detect GFP expression by immunohistochemistry (IHC) staining in regions that formed a polarized and specialized epithelium (Figure 1B). GFP expression was restricted to those intestinal tissues that uniformly stained positive for CDX2 and VIL1 (Figures 1B, S1C, and S1D), and a subset of cells stained positive for intestinal markers mucin 2 (MUC2), lysozyme (LYZ), chromogranin A (CHGA), and at a lower frequency for PDX1 (Figure 1B, S1C, and S1D). No significant GFP-positive staining in any other tissue type present in the teratoma, such as neuronal rosettes, cartilage, and smooth muscle, was detected (Figure S1C). Further, we could only detect GFP-positive cells in teratomas derived from LGR5-GFP$^{N\text{-term}}$ (n = 3) by IHC, and not in those derived from wild-type cells (n = 3) or LGR5-GFP$^{C\text{-term}}$ cells (n = 3), although those cells did functionally sort by fluorescence-activated cell sorting (FACS). These observations may suggest a functional difference between the two reporter systems, or they may reflect differential stability, processing, or localization of the LGR5-GFP fusion protein.

Isolation of Intestinal Organoids from LGR5-GFP hPSCs

The detection of LGR5-GFP-positive cells in teratomas prompted us to isolate these cells and test their ability to generate intestinal organoid cultures. We dissociated teratomas derived from LGR5-GFP hPSCs to a single-cell suspension and used FACS to isolate individual cells based on their GFP expression (Tables 1, top, and S2B). LGR5-GFP-positive cells were embedded in Matrigel and cultured in conditions previously described for human intestinal

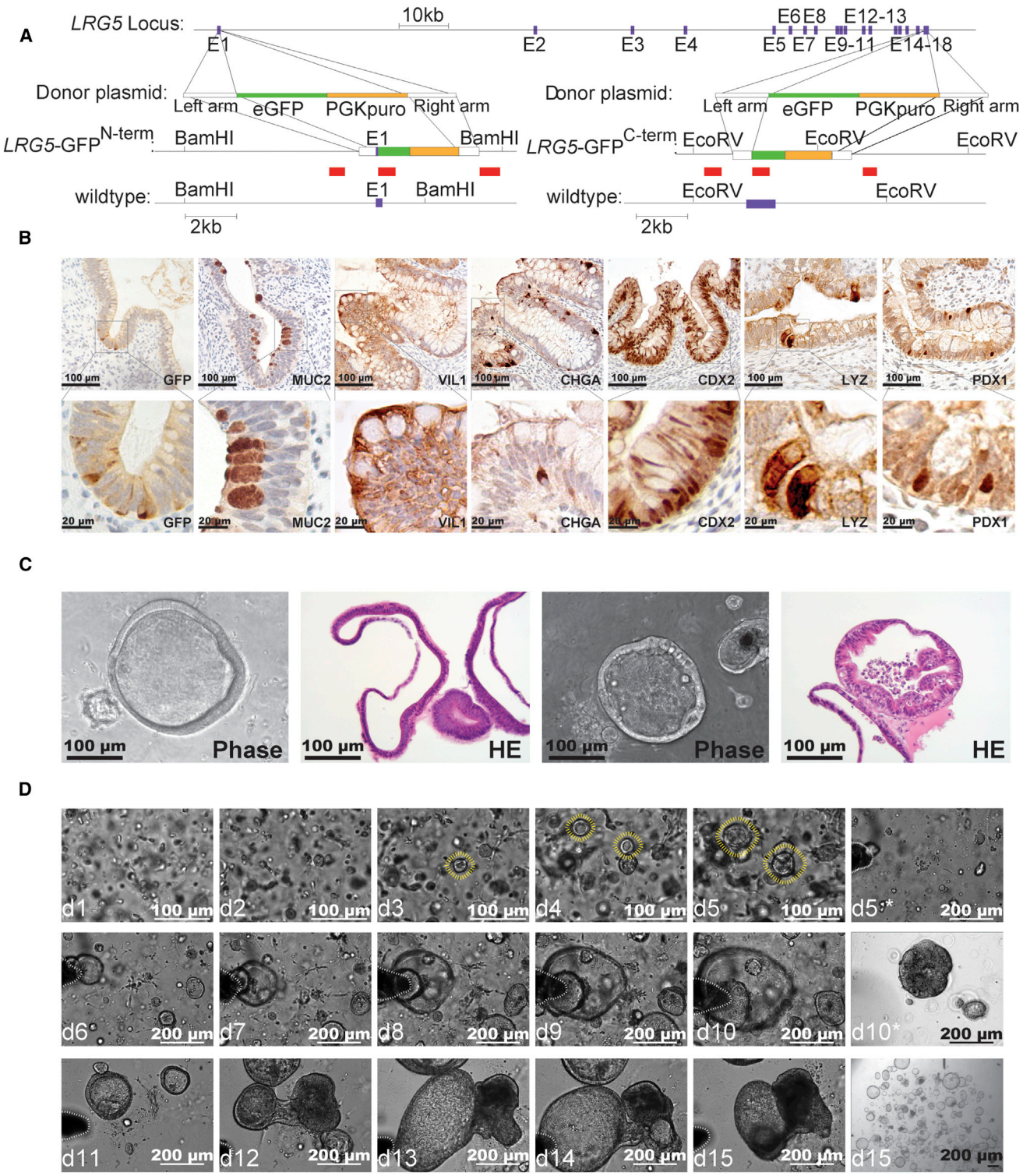

Figure 1. Generation of LGR5-GFP Reporter hESCs Using ZFNs

(A) Schematic overview depicting the gene-editing strategy for the LGR5 locus using a ZFN targeted to either the first or last coding exon of LGR5. Southern blot probes are shown as red boxes, exons are shown as blue boxes. Below are the donor plasmids used to target the LGR5 locus to generate either an N-terminal (LGR5-GFP$^{N\text{-term}}$) or a C-terminal (LGR5-GFP$^{C\text{-term}}$) LGR5-GFP reporter. pA, polyadenylation sequence;

(legend continued on next page)

Table 1.

WIBR3-hESC Derived

Teratoma-derived organoids[a]

		GFP Negative		GFP Positive			Total	
Teratomas	No. of organoids formed	No. of cells sorted	Cells forming organoids (%)	No. of organoids formed	No. of cells sorted	Cells forming organoids (%)	No. of cells sorted	Cells forming organoids (%)
Lgr5-GFP N-term	0	1,000	0	23	1,000	2.3	~50	>50,000	<0.1%
Lgr5-GFP N-term	0	1,710	0	101	1,710	5.91	~50	>50,000	<0.1%
Lgr5-GFP N-term	0	1,675	0	21	1,675	1.25	~50	>50,000	<0.1%
Lgr5-GFP C-term	0	4,203	0	38	4,203	0.9	~50	>50,000	<0.1%
Lgr5-GFP C-term	0	6,613	0	81	6,613	1.22	~50	>50,000	<0.1%
Lgr5-GFP N-term	0	6,046	0	3	6,046	0.05	~50	>50,000	<0.1%

Organoid-rederived organoids[b]

		GFP Negative		GFP Positive			Total	
Organoids	No. of organoids formed	No. of cells sorted	Cells forming organoids (%)	No. of organoids formed	No. of cells sorted	Cells forming organoids (%)	No. of cells sorted	Cells forming organoids (%)
Lgr5-GFP N-term	0	1,500	0	7	1,500	0.47	7	15,000	0.05
Lgr5-GFP N-term	24	6,700	0.36	140	6,700	2.09	65	13,000	0.5
Lgr5-GFP N-term	3	7,960	0.04	20	7,960	0.26	15	38,450	0.04

[a]Six independent teratomas FAC-sorted and assayed for organoid formation.
[b]Three organoids derived from three independent unsorted teratomas (dissociated, FAC-sorted, and assayed for organoid formation).

organoid cultures (Jung et al., 2011; Sato et al., 2011a, 2011b; Spence et al., 2011; Wang et al., 2013). Under these conditions, we observed multicellular epithelial structures with a central lumen after 3 days that proliferated into uniform, long-lived organoids with a morphology previously described for human intestinal organoids isolated from primary tissue (Fordham et al., 2013; Jung et al., 2011; Sato et al., 2011a; Figures 1C, 1D, S1E, and S4A–S4D).

It is important to note that in independent experiments, these organoids were generated with high frequency from GFP-positive cells (Table 1, top), although they could also be robustly generated from nonsorted teratoma cells by enrichment through serial passage (Figure 1D). Undifferentiated hESCs (Figure S4A) as well as the sorted GFP-negative fraction failed to give rise to organoids (Table 1, top), although this does not exclude the possibility that LGR5-negative cells could give rise to organoids under alternative conditions. The most prominent nonorganoid cells found to grow in the 3D matrix, regardless of whether the cells were GFP sorted or not, were single cells with neuronal precursor morphology. These contaminating cells were removed at each passage, enriching for nearly homogeneous long-term (>150 days) organoid cultures that could be maintained regardless of whether they were derived

PGK, phosphoglycerate kinase promoter; Puro, puromycin resistance gene; eGFP, enhanced green fluorescent protein. Shown below the donor plasmids is the LGR5 locus after targeting with the respective donor plasmids.
(B) IHC staining for indicated proteins in teratoma sections derived from LGR5-GFP$^{N\text{-}term}$ hESC reporter cells. MUC2, mucin2; VIL1, villin1; CHGA, chromogranin A; CDX2, caudal type homeobox 2; LYZ, lysozyme; PDX1, pancreatic and duodenal homeobox 1.
(C) Phase contrast and H&E staining of epithelial organoid cultures arising from LGR5-GFP sorting experiments. See quantification in Table 1.
(D) Bright-field images of developing organoids (outlined by yellow lines) derived from nonsorted single-cell suspensions after Matrigel embedding. The demarcation outlined by white lines in bright-field images taken on days 5*–15 was used as a reference point for tracking organoids clustered near this region. Cells were passaged every 5 days; here, an image before and after (*) passaging is shown. All bars, 200 μm.
See also Figure S1.

from GFP-positive cells or from nonsorted teratomas (Figures 1C, 1D, and S4A–S4D).

hPSC-Derived Intestinal Organoids Comprise All Major Cell Types of the Intestine

To characterize hPSC-derived intestinal organoids, we performed quantitative RT-PCR (qRT-PCR) analysis of cultures derived from GFP-FACS experiments, as well as from nonsorted teratoma cells, followed by RNA-seq analysis of samples of tissues from different stages of our differentiation paradigm and primary intestinal biopsy-derived organoids (Table S1). These analyses revealed the specific upregulation of intestinal stem cell markers such as LGR5, KLF5, and SOX9, and intestine-specific genes such as VIL1, MUC2, and TFF3 (Figures S5E and S5F). Marker gene expression for FGF8 and other nonintestinal cell types such as Nestin and Sox1 (both neural) and MIXL1 (mesoderm) was significantly decreased in hPSC-derived intestinal organoids. Genes that were not associated with high intestinal stem cell expression showed low and variable expression levels in the GFP-sorted organoids, and pluripotency genes such as Nanog were absent. These data indicate that hESC-derived organoids were no longer pluripotent, had an intestinal expression pattern, and could be isolated without LGR5-GFP sorting (Figures 2, S2A, and S5F). Organoid cultures failed to form tumors when injected subcutaneously into immunocompromised mice (data not shown).

We found a nearly identical expression profile between organoid cultures that had been generated using either the LGR5-GFP marker or unsorted teratoma cells, suggesting that our culture method was selective for intestinal stem/progenitor cells, and that although the LGR5-GFP reporter was functional, it was dispensable for isolating intestinal organoid cultures by this method. These observations indicate that our protocol may be generalized to other genetically engineered hPSCs without the LGR5 reporter.

The major differentiated cell types of the intestinal epithelium include Paneth cells, enterocytes, goblet cells, and enteroendocrine cells. We asked whether these cell types could also be detected in our hPSC-derived intestinal organoids. IHC analysis showed that the hPSC-derived organoids comprise a mostly polarized epithelium that includes differentiated cell types with distinct morphologies and specific marker gene expression (Figure 3). We identified cells with robust expression of CHGA, a marker for enteroendocrine cells; MUC2, a marker for goblet cells; and VIL1, which marks the villi of enterocytes (Figure 3). Furthermore, we observed a subset of organoids containing cells that were enriched for lysozyme staining (Figure S3; Movie S1).

The expression of adult intestinal marker proteins for the major cell types of the adult intestinal tissue prompted us to further analyze the composition and subcellular organization of hESC-derived organoids by electron microscopy (EM). Micrographs showed that organoids were organized in a polarized epithelium, with nuclei positioned proximal to the basolateral membrane (Figure 4A). The apical cellular membranes were characteristic of enterocytes with highly organized microvilli (Figures 4B-II and 4D-III) and tight junctions connecting neighboring enterocyte-like cells (Figures 4B-I and 4D-III). Goblet-shaped secretory cells (Figure 4C) that contained large vesicles coming from a well-defined rough endoplasmic reticulum (Figures 4D-I and 4D-II) were embedded in the enterocytes. Vesicles of these cells were localized at the apical side of the cell, suggesting secretion toward the lumen of the organoid (Figure 4).

hPSC-Derived Intestinal Organoids Contain Cells with Characteristics of Adult Intestinal Stem Cells

Adult stem cells have the ability to self-renew and a restricted capacity to differentiate into defined cell types. The human intestinal epithelium is a highly proliferative tissue with a turnover rate of ~5 days in differentiated cells outside the crypt. We found that single-cell-derived intestinal organoids could be maintained in long-term cultures (>6 months), suggesting the presence of a self-renewing cell population. To further test for the presence of such adult stem cell-like cells, we assayed for the minimum growth factors required to establish and maintain the organoid cultures. As expected for a system that originates from adult intestinal stem cells, we found a phenotypic growth dependence on epidermal growth factor (EGF), Noggin, and RSPO1 (ENR; Figures 5A and 5B), factors that are also essential in the mouse organoid system and human primary cultures (Barker et al., 2007; Sato et al., 2009; Spence et al., 2011). Alternative conditions that were previously reported to support human organoid cultures (Jung et al., 2011; McCracken et al., 2011; Spence et al., 2011; Wang et al., 2013) also allowed us to derive organoids from teratoma samples with a morphology similar to that described in previous studies (Finkbeiner and Spence, 2013; Sato et al., 2009; Stelzner et al., 2012; Figures S4B and S4C).

To further validate the presence of cells with adult stem cell-like characteristics in hPSC-derived intestinal organoids, we took advantage of the LGR5-GFP reporter system. First, we isolated organoid cultures from LGR5-GFP-derived teratomas without FACS sorting for GFP. After maintaining these cells for 5 days in 3D cultures, we investigated whether LGR5-GFP-positive cells were still present and able to form organoids after single-cell dissociation. We found that sorting for GFP fluorescence enriched for cells competent to form organoids when compared with the GFP-negative cell fraction (Table 1). Since LGR5 in mice marks intestinal stem, but not differentiated, cell types, this finding suggested that our culture conditions maintained cells with adult stem cell properties sufficient to

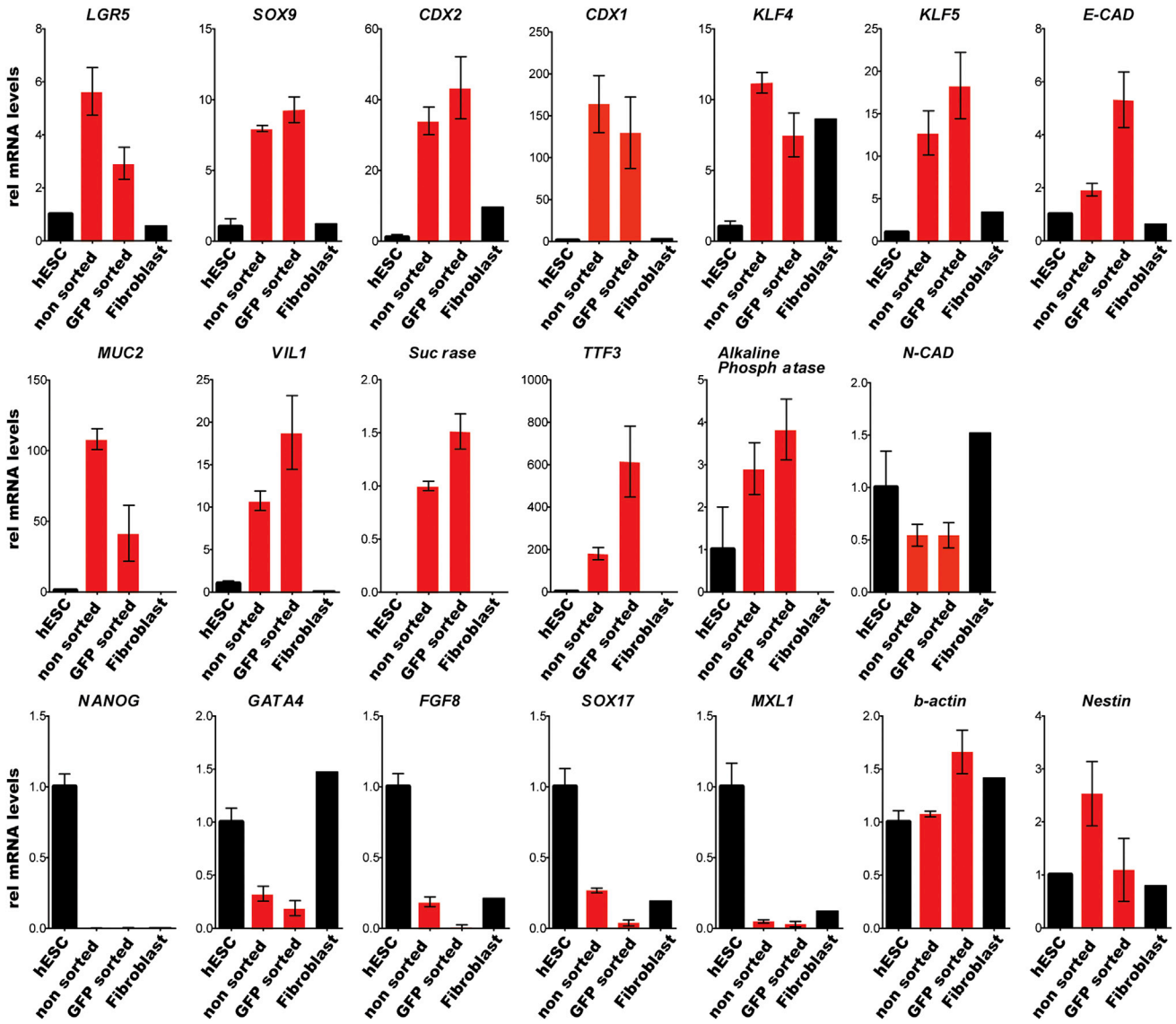

Figure 2. Isolation of Intestinal Organoids Independent of the LGR5-GFP Reporter System

Expression profiling of organoids from GFP-positive and nonsorted LGR5-GFP teratoma cells compared with hESCs and fibroblast-like cells. qRT-PCR for the indicated genes in hESCs, organoids derived from eGFP-positive cells (n = 3), and nonsorted (n = 3) cells of LGR5-GFP$^{N\text{-term}}$, hESCs, and fibroblast-like cells (derived from hESCs as described previously [Hockemeyer et al., 2008], expressing telomerase from the AAVS1 locus). Relative expression levels were normalized to baseline expression of these genes in hESCs. Data are biological replicates of independent experiments; bars represent the SEM. See also Figure S2.

form new organoids from single cells (Table 1; Figures 1D and S1).

To further substantiate the presence of functional adult stem cell-like cells in the hPSC-derived organoid system, we cultured hPSC-derived organoids under conditions known to either promote self-renewal (high WNT signaling) or induce differentiation (Notch inhibition) of intestinal stem cells. We found that reduced WNT signaling by withdrawal of either WNT or RSPO1 reduced proliferation and decreased expression of the stem cell markers LGR5 and OLFM4 (Figures 5C and 5D), and induced differentiation into secretory cells as indicated by a shift in cellular morphology detected by EM and immunofluorescence (IF) staining (Figure 5E and 5F). These cells showed an increased number of vesicles at the apical/luminal border (Figure 5E), maintained CDX2, increased MUC2, and a density of filamentous actin at the apical border by IF (Figures 4, 5E, and 5F).

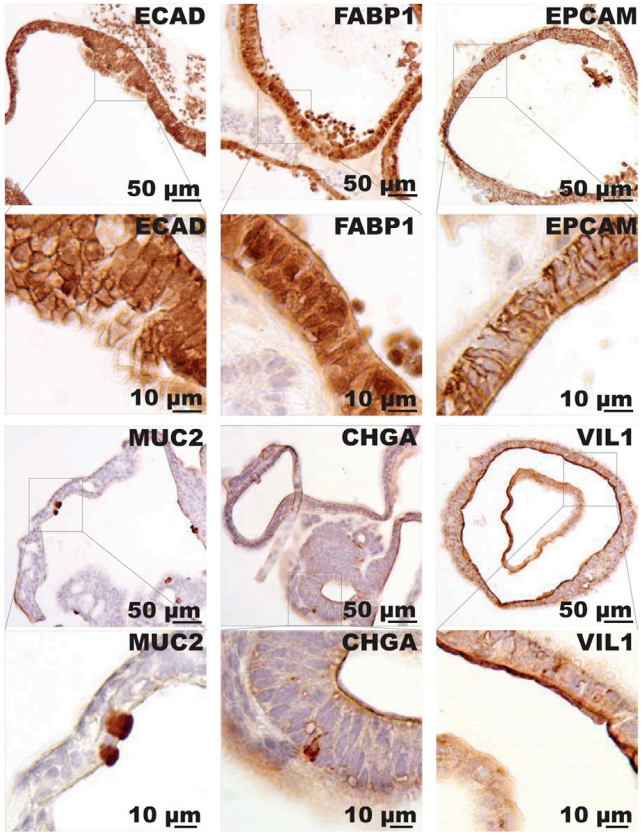

Figure 3. hESC-Derived Organoids Comprise Specific Cell Types Characteristic of the Human Intestinal Epithelium

(A) IHC staining for intestinal marker proteins in sections of hESC-derived organoids generated from wild-type hESC reporter cells. ECAD1, E-cadherin; FABP1, fatty acid-binding protein 1; EPCAM, epithelial cell adhesion molecule; MUC2, mucin2; CHGA, chromogranin A; VIL1, villin1.

See also Figure S3.

Long-term maintenance of adult stem cells requires telomerase expression and enzymatic activity (Günes and Rudolph, 2013). Telomerase activity in the human intestine is restricted to the stem cell compartment and is silenced upon differentiation of these cells (Schepers et al., 2011). We found that hPSC-derived organoid cultures could be maintained for several months, suggesting the presence of a self-renewing cell type. To functionally test whether hPSC-derived organoids contained telomerase-positive cells, we measured telomerase in vitro. As a positive control, we confirmed that the high level of telomerase activity in hESCs was significantly downregulated upon differentiation into fibroblast-like cells (Figure 5G). Notably, we could detect robust telomerase activity in three out of four independently derived intestinal organoid cultures when grown under adult stem cell conditions by telomeric repeat amplification protocol (TRAP) assay (Kim and Wu, 1997; Figure 5G). However, this activity was abrogated upon terminal differentiation of organoids by WNT-signaling withdrawal and inhibition of γ-secretase by DAPT. These functional data suggest that cells with adult stem cell properties, such as self-renewal and multipotency, represent a subpopulation of organoid cells that can respond appropriately to differentiation cues.

hPSC-Derived Intestinal Tissue Organoids Are Closely Related to Human Primary Intestinal Tissue-Derived Organoids

To determine the degree to which hPSC-derived organoids could recapitulate primary cultures established from adult intestinal tissue, we evaluated the expression profile using next-generation RNA-seq of hPSC-derived intestinal organoids cultured in media that either supported stem cell maintenance (n = 10) or induced terminal differentiation (n = 4). We compared these organoids with the parent hESC lines (n = 4) and teratoma samples (n = 4), and with organoids generated from adult human tissue samples biopsied from the duodenum (n = 2), ileum (n = 2), or rectum (n = 2). Unbiased complete linkage clustering for the top 5,000 most differentially expressed transcripts across these samples revealed that hESC-derived organoids closely resembled organoids isolated from the intestines of human subjects (Figures 6A and S5A). In contrast, teratoma samples were most similar to hESCs (Figures 6A, S5A, and S5C). Transcriptional profiling of organoids derived from an independent hESC line (BG01) confirmed that organoids could be derived irrespective of the genetic background of the hPSC cell line with high similarity to primary tissue-derived organoids (Figures 6A, 6B, and S5A–S5D). hESC-derived intestinal organoids grown in WENR (Wnt3a, EGF, Noggin, R-spondin-1) media expressed levels of intestinal adult stem cell marker genes (LGR5, OLFM4, KLF4, KLF5, SOX9, and TERT) and differentiated/secretory linage genes (e.g., KRT20, VIL1, MUC2, LYZ, CA2, SI, and PLA2GA) analogous to those found in organoids derived from primary tissue, with the greatest similarity to rectum-derived samples (Figures 6B, 6E, and S5D–S5G).

In contrast to previous results obtained by established protocols, our intestinal organoids did not result in a significant budding of crypt-like structures, which are characteristic of mouse small intestine cultures. The cystic morphology of our organoids was previously described for developmental immature stages of enterosphere differentiation, as well as for adult colon-derived organoids (Fordham et al., 2013; Jung et al., 2011; Sato et al., 2009; Stelzner et al., 2012). Whereas the expression levels of several marker proteins for intestinal function, such as PLAG2A, TFF1, and TFF2 (Figures S5D–S5F) offer evidence

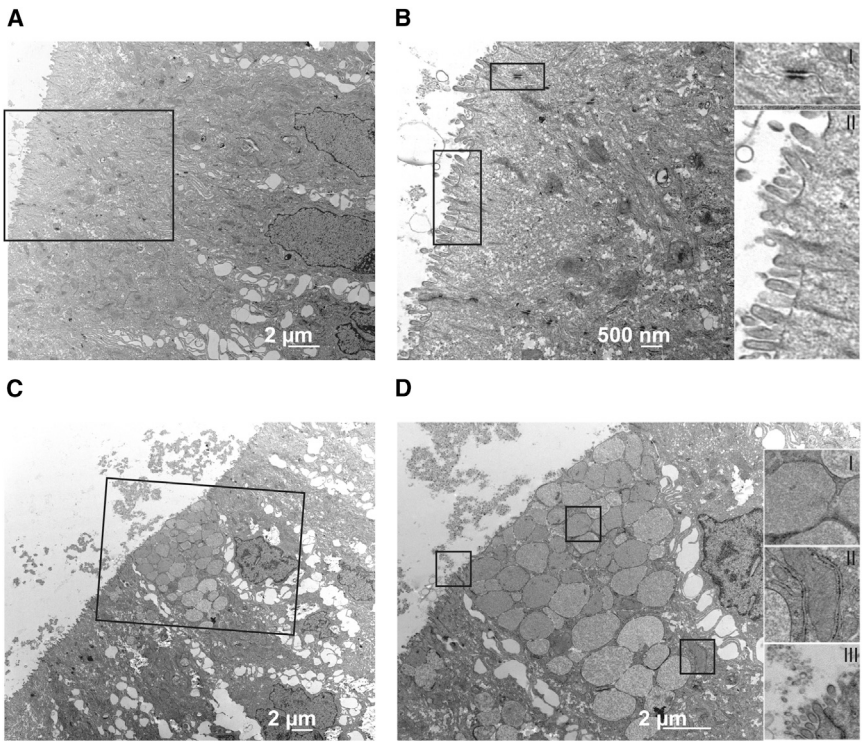

Figure 4. Subcellular Organization of Organoids Resembles the Structure of the Human Intestinal Epithelium

(A) Electron micrograph of hESC-derived organoids. Shown is a representative image with enterocyte-like cells forming a polarized epithelium. The lumen of the organoid is oriented to the left (apical), while the nuclei are aligned along the right (basal).

(B) Higher-magnification images of the micrograph shown in (A). Insets indicate areas of increased magnification. Images show the microvilli lining the luminal cell surface, vesicles in the luminal space (II), and the tight junctions connecting adjacent enterocyte-like cells (I).

(C) Electron micrograph of hESC-derived organoids. Shown is a representative image of a goblet-like secretory cell that is embedded into a sheet of enterocyte-like cells. Orientation of the image as in (A).

(D) Higher-magnification images of the micrograph shown in (C). Insets indicate areas of increased magnification. Images show magnification of vesicles (I), rough endoplasmic reticulum at the base of the vesicles (II), and tight junctions and cellular debris shed into the organoid's lumen (III).

of cell maturation of hESC-derived organoids, the full complexity of intestinal maturation was not recapitulated by this in vitro culture. The complex maturation signals required from the neural and vascular plexus and the mesenchyme have yet to be defined in an in vitro culture (Wells and Spence, 2014). Nevertheless, our protocol results in organoids that express adult stem cell markers to the same extent as primary tissue-derived organoids, suggesting that they are beyond a developmental stage that was recently described for human embryonic-like intestinal progenitor cells (Fordham et al., 2013; Figures S5B and S5D–S5F).

Next, we attempted to address the positional identity of these organoids with respect to anterior/posterior gut development. We found expression of the caudal-type homeobox gene CDX1 and the hindgut markers CDX2 (Sherwood et al., 2009) PLA2G2A, CA2, and MUC2 in hPSC-derived organoids and in rectum-derived tissues (Figures 6, S5D, and S5E). The midgut gene PDX1 was enriched in duodenal-derived samples only, and organoids expressed levels more comparable to the distal gut (ileum/rectum; Figure 6B). This analysis suggests that our differentiation protocol may bias for relatively mature hindgut/large intestinal-like tissue.

To further substantiate that hESC-derived organoids specifically express intestinal adult stem cell markers, we analyzed the expression profile of the LGR5-GFP reporter gene in hESC-derived organoids by RNA-seq. Here we found that both the LGR5-GFP$^{N\text{-term}}$ and LGR5-GFP$^{C\text{-term}}$ reporter recapitulated the expression of the endogenous LGR5 gene and contained a sequence that aligned across the expected fusion junction by RNA-seq (Figures 1A and 6C). Although the LGR5 reporter was expressed in hESCs and slightly reduced in teratoma cells, it was higher in the bulk analysis of organoids that were maintained under stem cell conditions. Importantly, LGR5-GFP expression was significantly repressed in organoid cultures under differentiation conditions (Figure 6C). These data not only validate our LGR5-GFP reporter systems, even though they showed minimal fluorescence by microscopy, but also support the hypothesis that a defined organoid system containing adult stem cells can be successfully generated from hPSCs by this method. Furthermore, a Gene Ontology analysis for genes that were differentially expressed between hESCs (n = 4) and hESC-derived intestinal organoids (n = 10) revealed a significant enrichment of genes associated with the gastrointestinal system (Figure 6D). Categories that were enriched included *Epithelial Differentiation* and *Digestion* for biological processes, and various *Peptidase Activities* for biological function. We also analyzed the genes that were differentially expressed between the human primary-derived samples and the

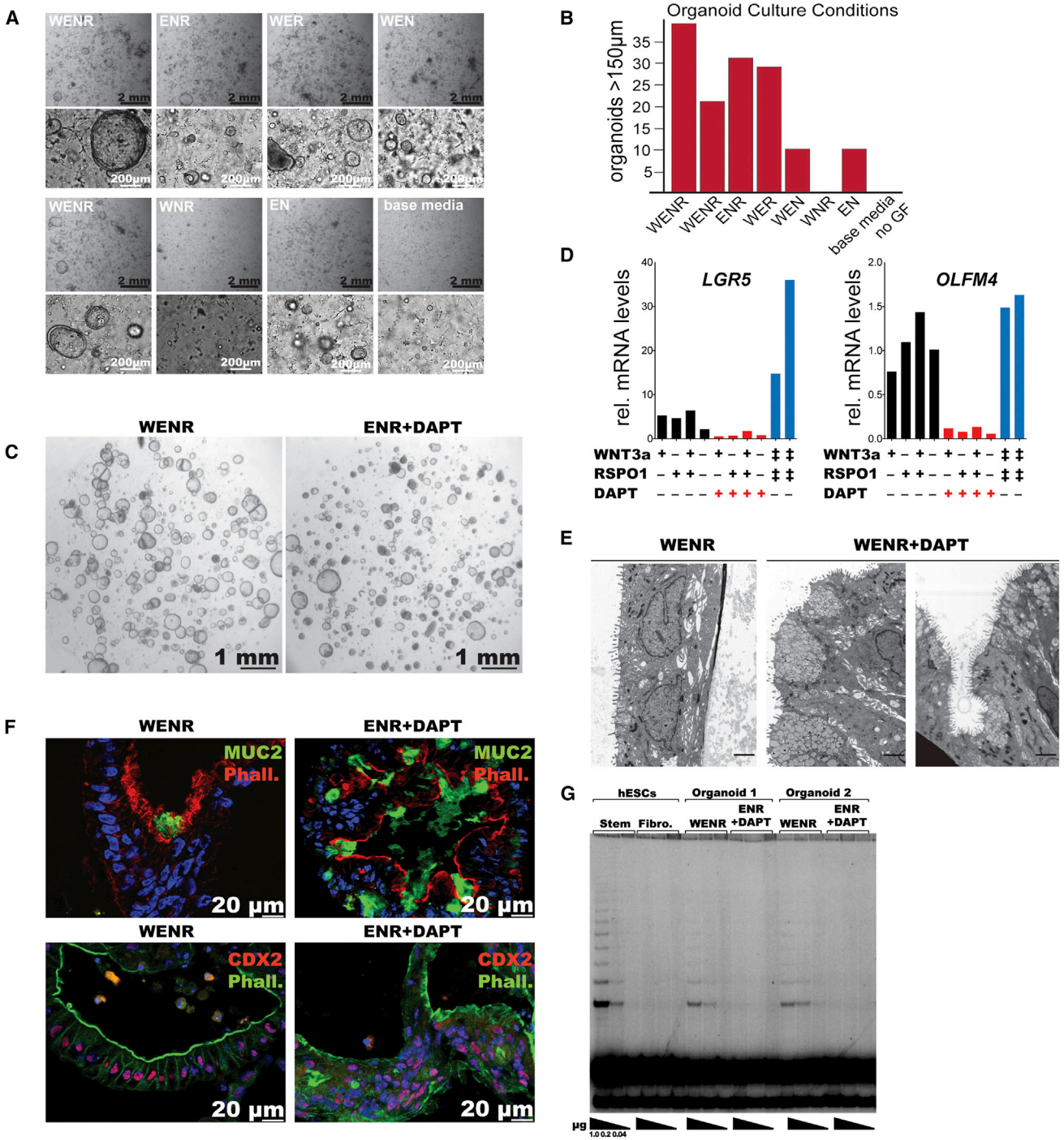

Figure 5. WNT and Notch Signaling Is Required to Establish and Maintain Cells with Adult Stem Cell Properties in hESC-Derived Intestinal Organoids

(A) Bright-field image of organoids at day 5 of their derivation under the indicated culture conditions at two different magnifications. Growth factors (GFs) : WENR [W, Wnt3a; E, EGF; N, Noggin; R, R-spondin-1] were supplemented in the combinations indicated. No GFs were added to "base media."

(B) Quantification of images shown in (A). The graph shows the number of organoids larger than 150 μm from a single teratoma isolation cultured in parallel under the conditions described in (A), where organoids were grown in 50 μl solidified Matrigel in 500 μl media/well in a 24-well plate.

(legend continued on next page)

hESC-derived organoids (see Supplemental Experimental Procedures for further discussion of the RNA-seq data).

Finally, we analyzed independently derived organoid cultures that were grown in the absence of WNT3a and in the presence of DAPT. Transcriptional changes showed that this specific change in WNT and Notch signaling resulted in the induction of intestinal-specific differentiation markers and a reduction of adult intestinal stem cell markers (Figures 6E and S5D).

In summary, our genome-wide expression analysis confirmed the following hypotheses: (1) organoids are similar to primary intestinal tissue, specifically the large intestine; (2) organoids express adult intestinal stem cell markers such as SOX9, OLFM4, KLF4, KLF5, LGR5, and TERT; (3) the genes expressed indicate that organoid cultures comprise a relatively mature hindgut-like tissue; (4) expression of LGR5 and the LGR5-GFP reporter is upregulated in mature organoids; and (5) organoids respond to the canonical cues that also determine differentiation and self-renewal in the intestine of adult humans.

DISCUSSION

A Human LGR5-GFP Reporter System Allows the Isolation of Intestinal Tissue Organoids

Here, we report on the development of a method that allows robust derivation of human intestinal adult stem cells and organoid tissue from hPSCs. We used ZFN-mediated genome editing of the endogenous LGR5 locus to generate a reporter system based on a previous study in mice that established LGR5 as a bona fide marker of adult intestinal stem cells (Barker et al., 2007). Analogous to what was observed in previous mouse experiments, we demonstrate here that generating either an N- or C-terminal reporter of human LGR5 allows the specific isolation and enrichment of cells with the ability to form organoid cultures from hPSCs despite showing minimal fluorescence by microscopy. Our results provide proof of concept for using site-specific gene-editing technology to isolate novel human cell types from hPSCs.

The intestinal organoids that we generated are similar to tissue isolated directly from humans, as they express gastrointestinal-specific genes and contain highly organized and differentiated cell types such as goblet-, enterocyte-, and enteroendocrine-like cells. In addition to the tissue organization, the cellular and subcellular morphology of hESC-derived organoids is reminiscent of primary organoid cultures. When grown under conditions that promote differentiation, organoids consist of an epithelial sheet of polarized cells with a subcellular organization characteristic of specific cell subtypes, such as secretory cells. Expression profiling suggests that our differentiation protocol may bias for relatively mature hindgut/large intestinal-like tissue. We do not know if this is an intrinsic feature of the teratoma or a function of our culture conditions. However, we find that a subset of organoids contain cells that stain positive for the small-intestine marker gene lysozyme, suggesting that our protocol does not strictly discriminate against more anterior regions of the intestine. As we can detect lysozyme- and PDX1-positive cells in the parent teratoma samples, it seems possible that our method could also be refined to specifically isolate and enrich for small-intestine cellular subtypes.

Modeling Intestinal Function and Disease Using hESC-Derived Intestinal Tissue

For many research applications, including nutrient uptake, drug delivery, metabolic regulation, and human disease modeling (e.g., intestinal cancer), rodent models do not fully recapitulate human intestinal physiology. However, organoids derived from hPSCs may provide a novel platform for in vitro disease modeling and drug screening to complement experiments in conventional animal models.

The organoid system established here will advance disease modeling because the differentiation protocol does

(C) Bright-field image of organoids at day 15. The image to the left shows a culture at day 15 when grown in WENR, and the right image shows the same cells when switched at day 10 to differentiation media.
(D) qRT-PCR for the intestinal stem cell markers LGR5 and OLFM4 in a single organoid culture treated in parallel with different culture conditions. The ‡ symbol indicates 1,000 ng/ml and 200 ng/ml of RSPO1 and WNT3a, respectively, and + indicates 200 μg/ml and 50 ng/ml of RSPO1 and WNT3a, respectively. Where indicated, DAPT was added at 10 μM.
(E) Electron micrographs of the cells shown in (C). Size bars indicate 2 μm.
(F) IF staining of cryosectioned organoids cultured in either stem cell media (WENR) or differentiation media (10 μM ENR+DAPT added for 4 consecutive days). Top: MUC2 (green), phalloidin (red), and DAPI (blue). Bottom: CDX2 (red), phalloidin (green), and DAPI (blue).
(G) TRAP assay (Kim and Wu, 1997) of hESCs, hESCs differentiated into fibroblast-like cells (Hockemeyer et al., 2008), intestinal organoids grown in stem cell media (WENR, n = 2) or differentiation media (10 μm ENR+ DAPT, n = 2). Shown is a ^{32}P autoradiogram of TRAP activity described for decreasing amounts of protein extracts (1.0–0.4 μg) for the indicated cell types (hESCs [WIBR3]; Fibro., fibroblast-like cells derived from WIBR3).
See also Figure S4.

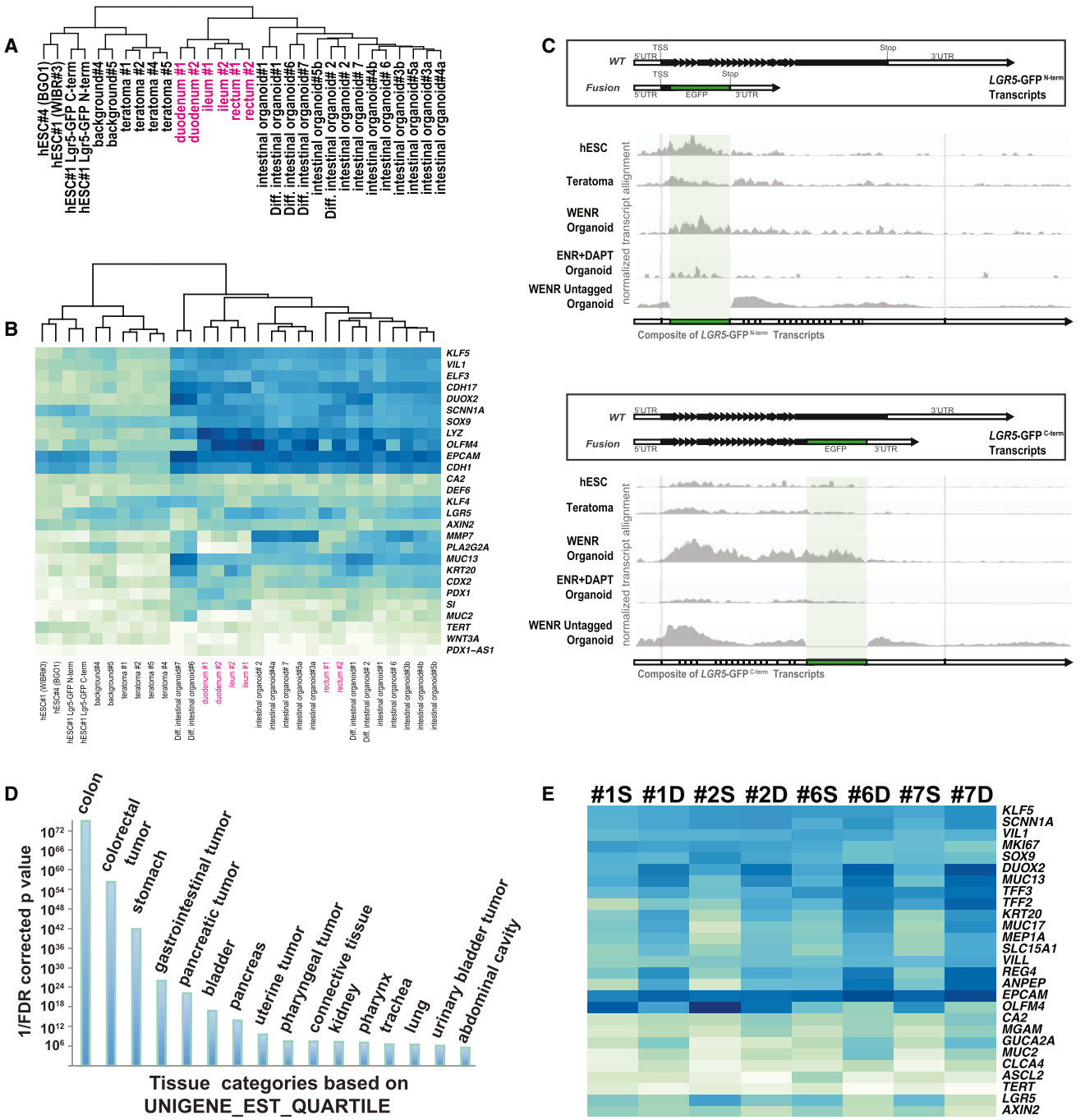

Figure 6. hESC-Derived Organoids Share a Transcriptional Profile with Primary Intestinal Tissue-Derived Organoids and Display the Characteristic Responses to Differentiation Stimuli

(A) Cluster analysis of hESCs (n = 4), teratoma samples (n = 4), bulk hESC-derived organoid cultures grown in WENR (n = 10), bulk cultures of hESC-derived organoids grown in differentiation medium (ENR+DAPT, n = 4), and primary duodenum- (n = 2), rectum- (n = 2) and ileum- (n = 2) derived organoids. Euclidian distances calculated from the abundance levels of the top 5,000 differentially expressed transcripts are also shown in Figure S1A.

(B) Heatmap displaying an unbiased cluster analysis of samples analyzed in (A) for a limited selection of genes relevant to intestinal expression and, in most cases, reported functions. Shown are the Euclidian distances calculated from the relative expression of the genes as determined by next-generation RNA-seq expression analysis.

(legend continued on next page)

not rely on the LGR5 reporter and because the committed intestinal stem cells can be derived from hiPSCs and hESCs. We demonstrate that hESCs that are genetically engineered by TALEN and ZFN-mediated genome editing can subsequently be used to generate intestinal organoids, suggesting that genome-editing approaches such as ZFN, TALEN, and CRISPR-mediated gene knockout and transgenesis will facilitate the study of intestinal biology. Gene editing will allow the generation of isogenic disease-specific cell lines, circumventing the problem of heterogeneity in human samples and eliminating the phenotypic heterogeneity of in vitro phenotypes (Soldner and Jaenisch, 2012; Soldner et al., 2011), thereby complementing current approaches that directly genetically modify intestinal organoid cultures (Miyoshi and Stappenbeck, 2013; Schwank et al., 2013).

hESC-Derived Organoids Represent a Novel In Vitro Adult Stem Cell System

Adult intestinal stem cells are a highly specialized and differentiated cell type that is formed through a well-timed and coordinated developmental process. Our isolation procedure for hPSC-derived intestinal adult stem cells suggests that these developmental cues can be sufficiently recapitulated when hPSCs form a teratoma. Key features of the differentiation process during teratoma formation that may allow for the establishment of adult stem cells include the extended period of time in which the tissue is allowed to form without perturbation, the optimal nutrient/hormonal conditions, and the unconstrained 3D growth in the subcutaneous compartment. In the future, these particular characteristics will have to be recapitulated in a xeno-free differentiation paradigm. Considering that LGR5 has recently also been implicated in adult stem cell function and maintenance of other tissue types, it will be interesting to investigate whether this strategy of genetically engineering hPSCs to carry reporter genes can be applied to the culture of other adult stem cell types that previously could not be isolated.

EXPERIMENTAL PROCEDURES

Teratoma Formation and Analysis

hESCs were collected by collagenase treatment (1.5 mg/ml) and separated from feeder cells by sedimentation. Cells were resuspended in 250 μl of PBS and injected subcutaneously into NOD-SCID mice (Taconic). All animal protocols were approved by the ACUC of UC Berkeley. Tumors (<1.5 cm) formed within 4–8 weeks, at which time teratomas were isolated and disaggregated to single cells or fixed in formalin for analysis of hematoxylin and eosin (H&E) staining. Immunostaining of paraffin sections was performed with standard techniques using a rabbit polyclonal anti-GFP antibody (Abcam 290).

Culture of Intestinal Epithelial Organoids from hESCs

Single cells isolated from teratomas were embedded at 4°C in 50 μl Matrigel containing 1 μM JAG-1 (No. 61298; AnaSpec) and incubated at 37°C for 10 min. The medium (500 μl/well) consisted of 1:1 Dulbecco's modified Eagle's medium F-12 and Neurobasic with N2, B27, L-glutamine, nonessential amino acids, penicillin/streptomycin, and growth factors WNT3A (200 ng ml^{-1}), RSPO1 (1 μg ml^{-1}), EGF (50 ng ml^{-1}), Noggin (100 ng ml^{-1}), and ROCK inhibitor (10 μM), and was changed every 2 days. Organoids were passaged using 5 min dispase digestion, subcultured, and gravity separated from single cells using a PBS 0.5% BSA wash. After a 5 min incubation in PBS, 0.5% BSA, and 2 mM EDTA, and hESC media inactivation, the tissue was pelleted and resuspended in 4°C Matrigel as described above. When indicated, WNT was withdrawn and 10 μM DAPT was added to the cultures for 4 days to induce differentiation.

Human Subject Tissues

The ethics committee of the University Medical Centre Utrecht approved this study and written informed consent was obtained from the human subjects. Organoids were generated from biopsies obtained for diagnostic purposes and maintained in culture (for 1–6 months) as described previously (Sato et al., 2011a).

IF Staining

Organoids were fixed in 3% paraformaldehyde with 5% sucrose in PBS (pH 7.4) for 30 min. Samples were embedded for cryosectioning, sectioned at 10 μM, and mounted on poly-L-lysine-coated

(C) Density maps of RNA-seq reads mapped to the genetically engineered LGR5-GFP$^{N\text{-term}}$ and LGR5-GFP$^{C\text{-term}}$ locus. The top boxes show the predicted transcripts for each allele based on validated gene editing described in Figure 1A. Shaded in green is the region mapping to the coding sequence for the eGPF fusion reporter. Shown across each histogram are the alignments to Lgr5-eGFP fusions predicted for each cell line. RNA was collected from the parent hESC cell lines, the intermediate teratoma samples, intestinal organoids, and intestinal organoids differentiated by the withdrawal of WNT3a and the addition of DAPT.

(D) Gene Ontology analysis for tissue-specific expression using the Database for Annotation, Visualization and Integrated Discovery (DAVID; http://david.abcc.ncifcrf.gov/home.jsp) and the "UNIGENE_EST_QUARTILE" expression profile database. Analyzed were genes significantly (FDR corrected p value < 0.05) unregulated (>$2^{2.5}$-fold) in hESC-derived intestinal organoids (n = 10) compared with hESCs (n = 4).

(E) Heatmap displaying an unbiased cluster analysis of organoid samples (from groups 1, 2, 6, and 7 as described in Table S1) analyzed in (A) for selected genes that are associated with the differentiation of adult intestinal stem cells. Shown are pairwise hESC-derived intestinal organoid cultures (n = 4) grown in either WENR stem cell media (S) or differentiated in ENR+DAPT (D).

See also Figure S5.

slides. Samples were permeabilized with TBST (Tris-buffered saline with 0.5% Triton X-100) and incubated at 4°C, 1:5,000 dilution, with shaking overnight. The slides were washed three times with TBST at 4°C and then incubated with the appropriate Alexa Fluor secondary antibodies (1:1,000) and a phalloidin conjugate (1:1,000). Afterward, the slides were washed as before, stained for DAPI, and mounted.

Transcriptional Profiling

Details regarding the protocol used for transcriptional profiling are provided in Supplemental Experimental Procedures. Briefly, an RNA-seq library was created using the standard Illumina library preparation protocol. Ribosomal RNAs were depleted using a oligo(dT) 25 magnetic bead kit (Life Technologies), and the libraries were generated using the PrepX SPIA RNA-Seq and PrepX Library kit (IntegenX) according to the manufacturer's protocol. Reads were mapped to the Ensembl cDNA release 72 (Flicek et al., 2013) with Bowtie2 version 2.1.0 (Langmead and Salzberg, 2012) using the parameters –rdg 6,5, –rfg 6,5, and –score-min L,-.6,-.4. Transcript abundances were calculated with eXpress version 1.4.0 (Roberts and Pachter, 2013) and the resulting effective counts for each transcript were used to calculate fold changes. Effective counts were also processed with DESeq version 1.12.0 (Anders and Huber, 2010) to identify statistically significant differentially expressed genes and transcripts. Fragments per kilobase of transcript per million mapped reads (FPKM) results are available in Supplemental Experimental Procedures and the raw data for RNA-seq are available at http://www.ncbi.nlm.nih.gov/geo/query/acc.cgi?acc=GSE56930.

Additional details regarding the methods used in this work can be found in Supplemental Experimental Procedures.

ACCESSION NUMBERS

The GEO accession number for the RNA-seq data reported in this paper is GSE56930.

SUPPLEMENTAL INFORMATION

Supplemental Information includes Supplemental Experimental Procedures, five figures, two tables, and one movie and can be found with this article online at http://dx.doi.org/10.1016/j.stemcr.2014.05.001.

ACKNOWLEDGMENTS

We thank R. Alagappan, P. Xu, Dong Dong Wu, and Lei Zhang and the Sangamo Production group for expert technical assistance. We thank Frank Soldner, Thomas Sandmann, and Helen Bateup for helpful comments during the design of the experiment. We thank Nicki Watson from the Keck Imaging Facility at the Whitehead Institute for performing the EM analysis. R.F. is supported by the National Science Foundation Graduate Research Fellowship Program (GRFP) under grant DGE 1106400 and NIH training grant 2T32GM007232-36. K.C. was supported by a fellowship from the Nakajima Foundation. R.J. was supported by NIH grants R37-CA084198, RO1-CA087869, and RO1-HD045022, and by a grant from the HHMI. R.J. is an adviser to Stemgent and a cofounder of Fate Therapeutics. D.H. is a New Scholar in Aging of the Ellison Medical Foundation and is supported by the Glenn Foundation and the Shurl and Kay Curci Foundation. G.J.C., A.C., E.J.R., P.D.G., and F.D.U. are full-time employees of Sangamo BioSciences.

Received: November 24, 2013
Revised: May 4, 2014
Accepted: May 5, 2014
Published: June 3, 2014

REFERENCES

Anders, S., and Huber, W. (2010). Differential expression analysis for sequence count data. Genome Biol. *11*, R106.

Barker, N., van Es, J.H., Kuipers, J., Kujala, P., van den Born, M., Cozijnsen, M., Haegebarth, A., Korving, J., Begthel, H., Peters, P.J., and Clevers, H. (2007). Identification of stem cells in small intestine and colon by marker gene Lgr5. Nature *449*, 1003–1007.

Cao, L., Gibson, J.D., Miyamoto, S., Sail, V., Verma, R., Rosenberg, D.W., Nelson, C.E., and Giardina, C. (2011). Intestinal lineage commitment of embryonic stem cells. Differentiation *81*, 1–10.

Carmon, K.S., Gong, X., Lin, Q., Thomas, A., and Liu, Q. (2011). R-spondins function as ligands of the orphan receptors LGR4 and LGR5 to regulate Wnt/beta-catenin signaling. Proc. Natl. Acad. Sci. USA *108*, 11452–11457.

de Lau, W., Barker, N., Low, T.Y., Koo, B.-K., Li, V.S.W., Teunissen, H., Kujala, P., Haegebarth, A., Peters, P.J., van de Wetering, M., et al. (2011). Lgr5 homologues associate with Wnt receptors and mediate R-spondin signalling. Nature *476*, 293–297.

DeKelver, R.C., Choi, V.M., Moehle, E.A., Paschon, D.E., Hockemeyer, D., Meijsing, S.H., Sancak, Y., Cui, X., Steine, E.J., Miller, J.C., et al. (2010). Functional genomics, proteomics, and regulatory DNA analysis in isogenic settings using zinc finger nuclease-driven transgenesis into a safe harbor locus in the human genome. Genome Res. *20*, 1133–1142.

Dekkers, J.F., Wiegerinck, C.L., de Jonge, H.R., Bronsveld, I., Janssens, H.M., de Winter-de Groot, K.M., Brandsma, A.M., de Jong, N.W.M., Bijvelds, M.J.C., Scholte, B.J., et al. (2013). A functional CFTR assay using primary cystic fibrosis intestinal organoids. Nat. Med. *19*, 939–945.

Finkbeiner, S.R., and Spence, J.R. (2013). A gutsy task: generating intestinal tissue from human pluripotent stem cells. Dig. Dis. Sci. *58*, 1176–1184.

Flicek, P., Ahmed, I., Amode, M.R., Barrell, D., Beal, K., Brent, S., Carvalho-Silva, D., Clapham, P., Coates, G., Fairley, S., et al. (2013). Ensembl 2013. Nucleic Acids Res. *41* (Database issue), D48–D55.

Fordham, R.P., Yui, S., Hannan, N.R., Soendergaard, C., Madgwick, A., Schweiger, P.J., Nielsen, O.H., Vallier, L., Pedersen, R.A., Nakamura, T., et al. (2013). Transplantation of expanded fetal intestinal progenitors contributes to colon regeneration after injury. Cell Stem Cell *13*, 734–744.

Günes, C., and Rudolph, K.L. (2013). The role of telomeres in stem cells and cancer. Cell *152*, 390–393.

Hockemeyer, D., Soldner, F., Cook, E.G., Gao, Q., Mitalipova, M., and Jaenisch, R. (2008). A drug-inducible system for direct

reprogramming of human somatic cells to pluripotency. Cell Stem Cell *3*, 346–353.

Hockemeyer, D., Soldner, F., Beard, C., Gao, Q., Mitalipova, M., DeKelver, R.C., Katibah, G.E., Amora, R., Boydston, E.A., Zeitler, B., et al. (2009). Efficient targeting of expressed and silent genes in human ESCs and iPSCs using zinc-finger nucleases. Nat. Biotechnol. *27*, 851–857.

Hockemeyer, D., Wang, H., Kiani, S., Lai, C.S., Gao, Q., Cassady, J.P., Cost, G.J., Zhang, L., Santiago, Y., Miller, J.C., et al. (2011). Genetic engineering of human pluripotent cells using TALE nucleases. Nat. Biotechnol. *29*, 731–734.

Jung, P., Sato, T., Merlos-Suárez, A., Barriga, F.M., Iglesias, M., Rossell, D., Auer, H., Gallardo, M., Blasco, M.A., Sancho, E., et al. (2011). Isolation and in vitro expansion of human colonic stem cells. Nat. Med. *17*, 1225–1227.

Kim, N.W., and Wu, F. (1997). Advances in quantification and characterization of telomerase activity by the telomeric repeat amplification protocol (TRAP). Nucleic Acids Res. *25*, 2595–2597.

Kim, K.-A., Kakitani, M., Zhao, J., Oshima, T., Tang, T., Binnerts, M., Liu, Y., Boyle, B., Park, E., Emtage, P., et al. (2005). Mitogenic influence of human R-spondin1 on the intestinal epithelium. Science *309*, 1256–1259.

Korinek, V., Barker, N., Moerer, P., van Donselaar, E., Huls, G., Peters, P.J., and Clevers, H. (1998). Depletion of epithelial stem-cell compartments in the small intestine of mice lacking Tcf-4. Nat. Genet. *19*, 379–383.

Langmead, B., and Salzberg, S.L. (2012). Fast gapped-read alignment with Bowtie 2. Nat. Methods *9*, 357–359.

Lengner, C.J., Gimelbrant, A.A., Erwin, J.A., Cheng, A.W., Guenther, M.G., Welstead, G.G., Alagappan, R., Frampton, G.M., Xu, P., Muffat, J., et al. (2010). Derivation of pre-X inactivation human embryonic stem cells under physiological oxygen concentrations. Cell *141*, 872–883.

McCracken, K.W., Howell, J.C., Wells, J.M., and Spence, J.R. (2011). Generating human intestinal tissue from pluripotent stem cells in vitro. Nat. Protoc. *6*, 1920–1928.

McDonald, T., Wang, R., Bailey, W., Xie, G., Chen, F., Caskey, C.T., and Liu, Q. (1998). Identification and cloning of an orphan G protein-coupled receptor of the glycoprotein hormone receptor subfamily. Biochem. Biophys. Res. Commun. *247*, 266–270.

Miyoshi, H., and Stappenbeck, T.S. (2013). In vitro expansion and genetic modification of gastrointestinal stem cells in spheroid culture. Nat. Protoc. *8*, 2471–2482.

Ogaki, S., Shiraki, N., Kume, K., and Kume, S. (2013). Wnt and Notch signals guide embryonic stem cell differentiation into the intestinal lineages. Stem Cells *31*, 1086–1096.

Ootani, A., Li, X., Sangiorgi, E., Ho, Q.T., Ueno, H., Toda, S., Sugihara, H., Fujimoto, K., Weissman, I.L., Capecchi, M.R., and Kuo, C.J. (2009). Sustained in vitro intestinal epithelial culture within a Wnt-dependent stem cell niche. Nat. Med. *15*, 701–706.

Pellegrinet, L., Rodilla, V., Liu, Z., Chen, S., Koch, U., Espinosa, L., Kaestner, K.H., Kopan, R., Lewis, J., and Radtke, F. (2011). Dll1- and dll4-mediated notch signaling are required for homeostasis of intestinal stem cells. Gastroenterology *140*, 1230–1240, e1–e7.

Roberts, A., and Pachter, L. (2013). Streaming fragment assignment for real-time analysis of sequencing experiments. Nat. Methods *10*, 71–73.

Ruffner, H., Sprunger, J., Charlat, O., Leighton-Davies, J., Grosshans, B., Salathe, A., Zietzling, S., Beck, V., Therier, M., Isken, A., et al. (2012). R-Spondin potentiates Wnt/β-catenin signaling through orphan receptors LGR4 and LGR5. PLoS ONE *7*, e40976.

Sato, T., Vries, R.G., Snippert, H.J., van de Wetering, M., Barker, N., Stange, D.E., van Es, J.H., Abo, A., Kujala, P., Peters, P.J., and Clevers, H. (2009). Single Lgr5 stem cells build crypt-villus structures in vitro without a mesenchymal niche. Nature *459*, 262–265.

Sato, T., Stange, D.E., Ferrante, M., Vries, R.G.J., Van Es, J.H., Van den Brink, S., Van Houdt, W.J., Pronk, A., Van Gorp, J., Siersema, P.D., and Clevers, H. (2011a). Long-term expansion of epithelial organoids from human colon, adenoma, adenocarcinoma, and Barrett's epithelium. Gastroenterology *141*, 1762–1772.

Sato, T., van Es, J.H., Snippert, H.J., Stange, D.E., Vries, R.G., van den Born, M., Barker, N., Shroyer, N.F., van de Wetering, M., and Clevers, H. (2011b). Paneth cells constitute the niche for Lgr5 stem cells in intestinal crypts. Nature *469*, 415–418.

Schepers, A.G., Vries, R., van den Born, M., van de Wetering, M., and Clevers, H. (2011). Lgr5 intestinal stem cells have high telomerase activity and randomly segregate their chromosomes. EMBO J. *30*, 1104–1109.

Schwank, G., Koo, B.K., Sasselli, V., Dekkers, J.F., Heo, I., Demircan, T., Sasaki, N., Boymans, S., Cuppen, E., van der Ent, C.K., et al. (2013). Functional repair of CFTR by CRISPR/Cas9 in intestinal stem cell organoids of cystic fibrosis patients. Cell Stem Cell *13*, 653–658.

Sherwood, R.I., Chen, T.Y., and Melton, D.A. (2009). Transcriptional dynamics of endodermal organ formation. Dev. Dyn. *238*, 29–42.

Snippert, H.J., van der Flier, L.G., Sato, T., van Es, J.H., van den Born, M., Kroon-Veenboer, C., Barker, N., Klein, A.M., van Rheenen, J., Simons, B.D., and Clevers, H. (2010). Intestinal crypt homeostasis results from neutral competition between symmetrically dividing Lgr5 stem cells. Cell *143*, 134–144.

Soldner, F., and Jaenisch, R. (2012). Medicine. iPSC disease modeling. Science *338*, 1155–1156.

Soldner, F., Laganière, J., Cheng, A.W., Hockemeyer, D., Gao, Q., Alagappan, R., Khurana, V., Golbe, L.I., Myers, R.H., Lindquist, S., et al. (2011). Generation of isogenic pluripotent stem cells differing exclusively at two early onset Parkinson point mutations. Cell *146*, 318–331.

Spence, J.R., Mayhew, C.N., Rankin, S.A., Kuhar, M.F., Vallance, J.E., Tolle, K., Hoskins, E.E., Kalinichenko, V.V., Wells, S.I., Zorn, A.M., et al. (2011). Directed differentiation of human pluripotent stem cells into intestinal tissue in vitro. Nature *470*, 105–109.

Stelzner, M., Helmrath, M., Dunn, J.C., Henning, S.J., Houchen, C.W., Kuo, C., Lynch, J., Li, L., Magness, S.T., Martin, M.G., et al.; NIH Intestinal Stem Cell Consortium (2012). A nomenclature for intestinal in vitro cultures. Am. J. Physiol. Gastrointest. Liver Physiol. *302*, G1359–G1363.

Takahashi, K., Tanabe, K., Ohnuki, M., Narita, M., Ichisaka, T., Tomoda, K., and Yamanaka, S. (2007). Induction of pluripotent stem cells from adult human fibroblasts by defined factors. Cell *131*, 861–872.

van Es, J.H., van Gijn, M.E., Riccio, O., van den Born, M., Vooijs, M., Begthel, H., Cozijnsen, M., Robine, S., Winton, D.J., Radtke, F., and Clevers, H. (2005). Notch/gamma-secretase inhibition turns proliferative cells in intestinal crypts and adenomas into goblet cells. Nature *435*, 959–963.

Wang, P., Rodriguez, R.T., Wang, J., Ghodasara, A., and Kim, S.K. (2011). Targeting SOX17 in human embryonic stem cells creates unique strategies for isolating and analyzing developing endoderm. Cell Stem Cell *8*, 335–346.

Wang, F., Scoville, D., He, X.C., Mahe, M.M., Box, A., Perry, J.M., Smith, N.R., Lei, N.Y., Davies, P.S., Fuller, M.K., et al. (2013). Isolation and characterization of intestinal stem cells based on surface marker combinations and colony-formation assay. Gastroenterology *145*, 383–395, e1–e21.

Wells, J.M., and Spence, J.R. (2014). How to make an intestine. Development *141*, 752–760.

Yui, S., Nakamura, T., Sato, T., Nemoto, Y., Mizutani, T., Zheng, X., Ichinose, S., Nagaishi, T., Okamoto, R., Tsuchiya, K., et al. (2012). Functional engraftment of colon epithelium expanded in vitro from a single adult $Lgr5^+$ stem cell. Nat. Med. *18*, 618–623.

Yusa, K., Rashid, S.T., Strick-Marchand, H., Varela, I., Liu, P.-Q., Paschon, D.E., Miranda, E., Ordóñez, A., Hannan, N.R.F., Rouhani, F.J., et al. (2011). Targeted gene correction of α1-antitrypsin deficiency in induced pluripotent stem cells. Nature *478*, 391–394.

Zou, J., Maeder, M.L., Mali, P., Pruett-Miller, S.M., Thibodeau-Beganny, S., Chou, B.K., Chen, G., Ye, Z., Park, I.H., Daley, G.Q., et al. (2009). Gene targeting of a disease-related gene in human induced pluripotent stem and embryonic stem cells. Cell Stem Cell *5*, 97–110.

Stem Cell Reports, Volume *2*

Supplemental Information

Human Intestinal Tissue with Adult Stem Cell Properties Derived from Pluripotent Stem Cells

Ryan Forster, Kunitoshi Chiba, Lorian Schaeffer, Samuel G. Regalado, Christine S. Lai, Qing Gao, Samira Kiani, Henner F. Farin, Hans Clevers, Gregory J. Cost, Andy Chan, Edward J. Rebar, Fyodor D. Urnov, Philip D. Gregory, Lior Pachter, Rudolf Jaenisch, and Dirk Hockemeyer

Figure S1

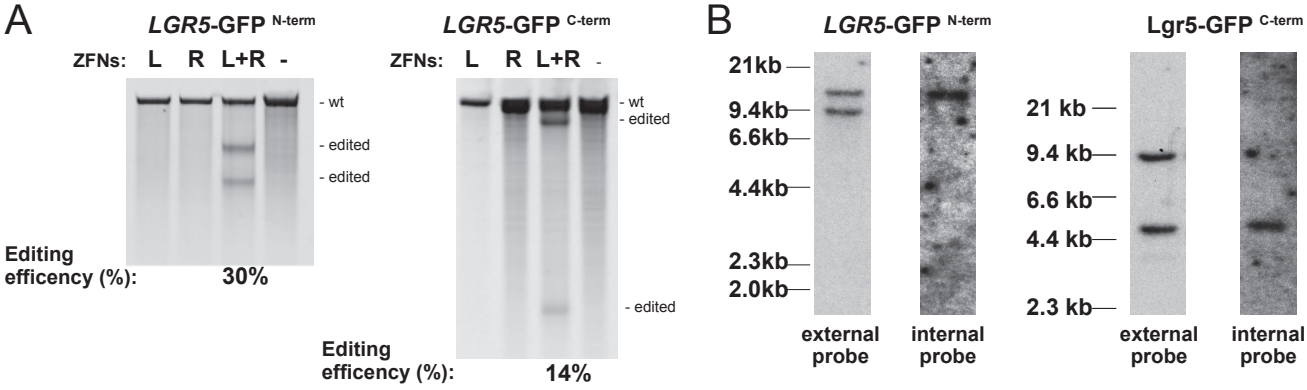
A
LGR5-GFP N-term
ZFNs: L R L+R -
- wt
- edited
- edited
Editing efficency (%): 30%
LGR5-GFP C-term
ZFNs: L R L+R -
- wt
- edited
- edited
Editing efficency (%): 14%
B
LGR5-GFP N-term
21kb
9.4kb
6.6kb
4.4kb
2.3kb
2.0kb
external probe
internal probe
Lgr5-GFP C-term
21 kb
9.4 kb
6.6 kb
4.4 kb
2.3 kb
external probe
internal probe

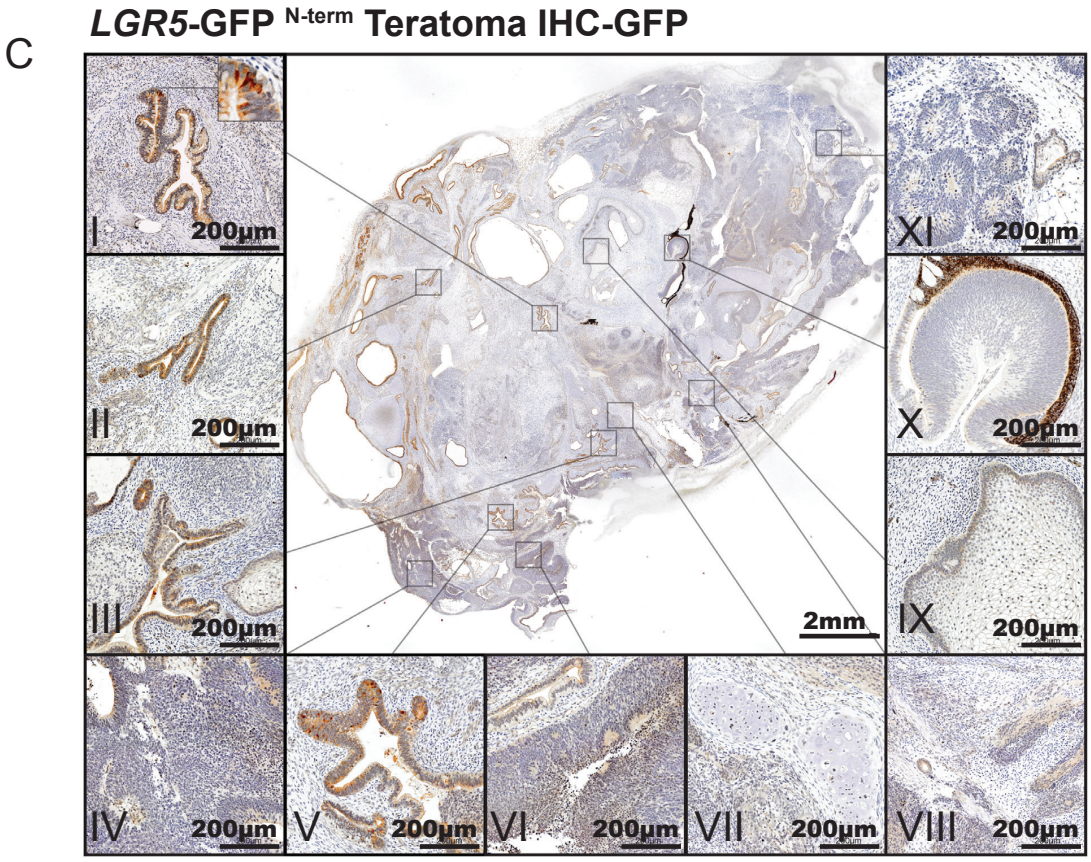
C
LGR5-GFP N-term Teratoma IHC-GFP
I 200µm
II 200µm
III 200µm
IV 200µm
V 200µm
VI 200µm
VII 200µm
VIII 200µm
IX 200µm
X 200µm
XI 200µm
2mm

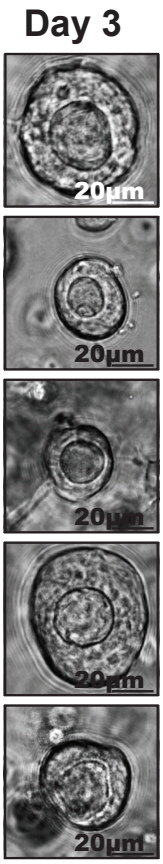
E
Day 3
20µm
20µm
20µm
20µm
20µm

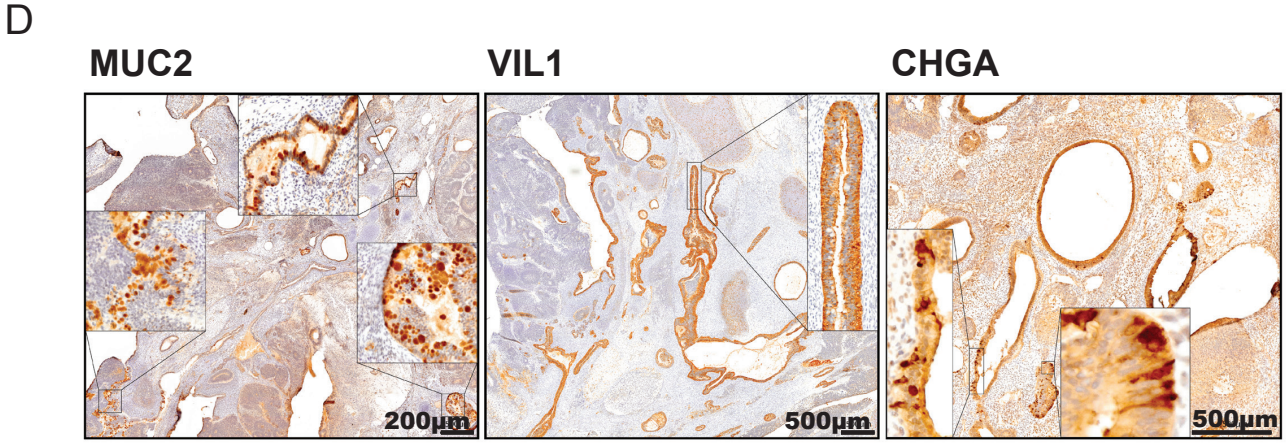
D
MUC2
VIL1
CHGA
200µm
500µm
500µm

Figure S2

A

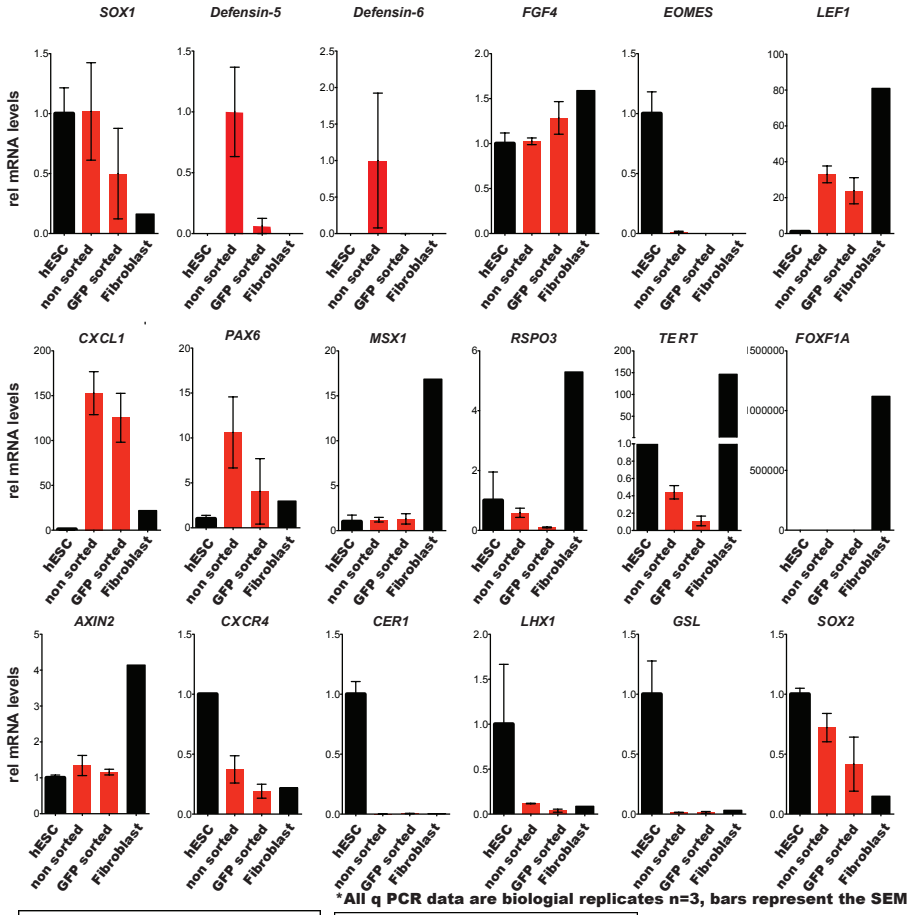

*All q PCR data are biologial replicates n=3, bars represent the SEM

B

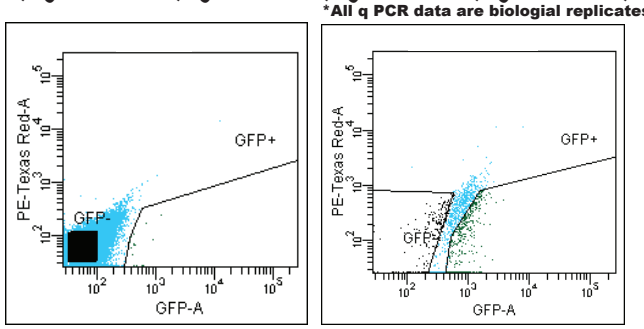

Tube: 1

Population	#Events	%Parent	%Total
All Events	50,000	####	100.0
Singlets	38,847	77.7	77.7
SSC Singlets	38,471	99.0	76.9
FSC Singlets	38,250	99.4	76.5
GFP+	16	0.0	0.0
GFP-	8,991	23.5	18.0

Tube: 11

Population	#Events	%Parent	%Total
All Events	4,178	####	100.0
Singlets	1,411	33.8	33.8
SSC Singlets	1,293	91.6	30.9
FSC Singlets	1,201	92.9	28.7
GFP+	340	28.3	8.1
GFP-	227	18.9	5.4

Figure S3

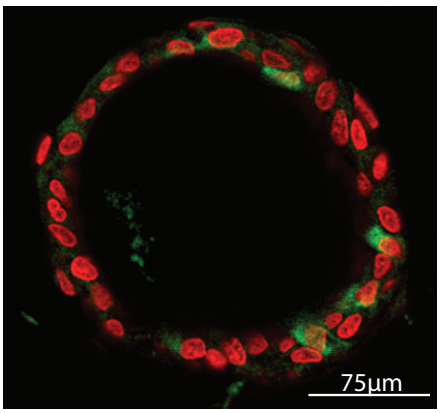

Figure S4

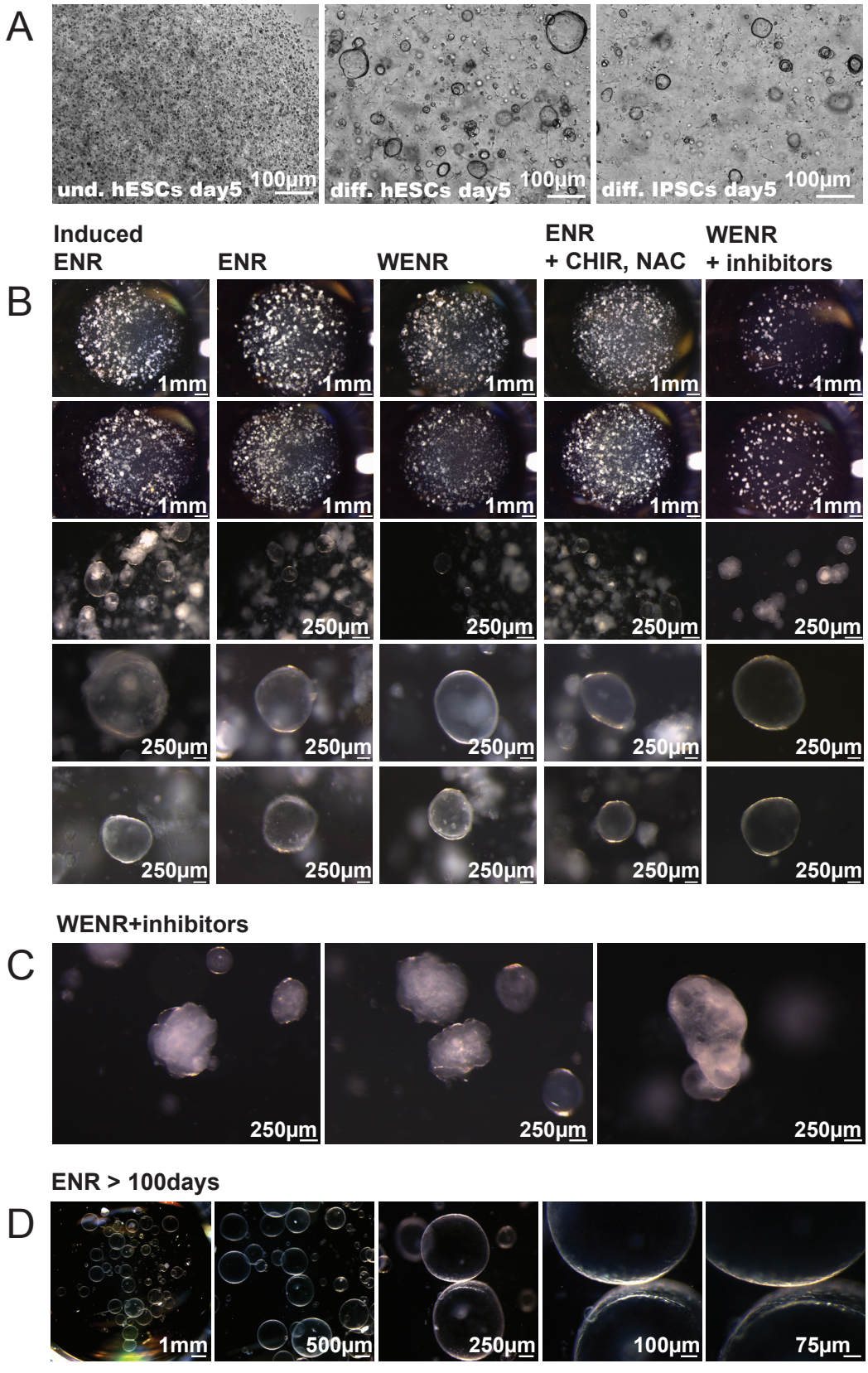
A
und. hESCs day5
100µm
diff. hESCs day5
100µm
diff. IPSCs day5
100µm
B
Induced ENR
ENR
WENR
ENR + CHIR, NAC
WENR + inhibitors
1mm
250µm
C
WENR+inhibitors
250µm
D
ENR > 100days
1mm
500µm
250µm
100µm
75µm

Figure S5

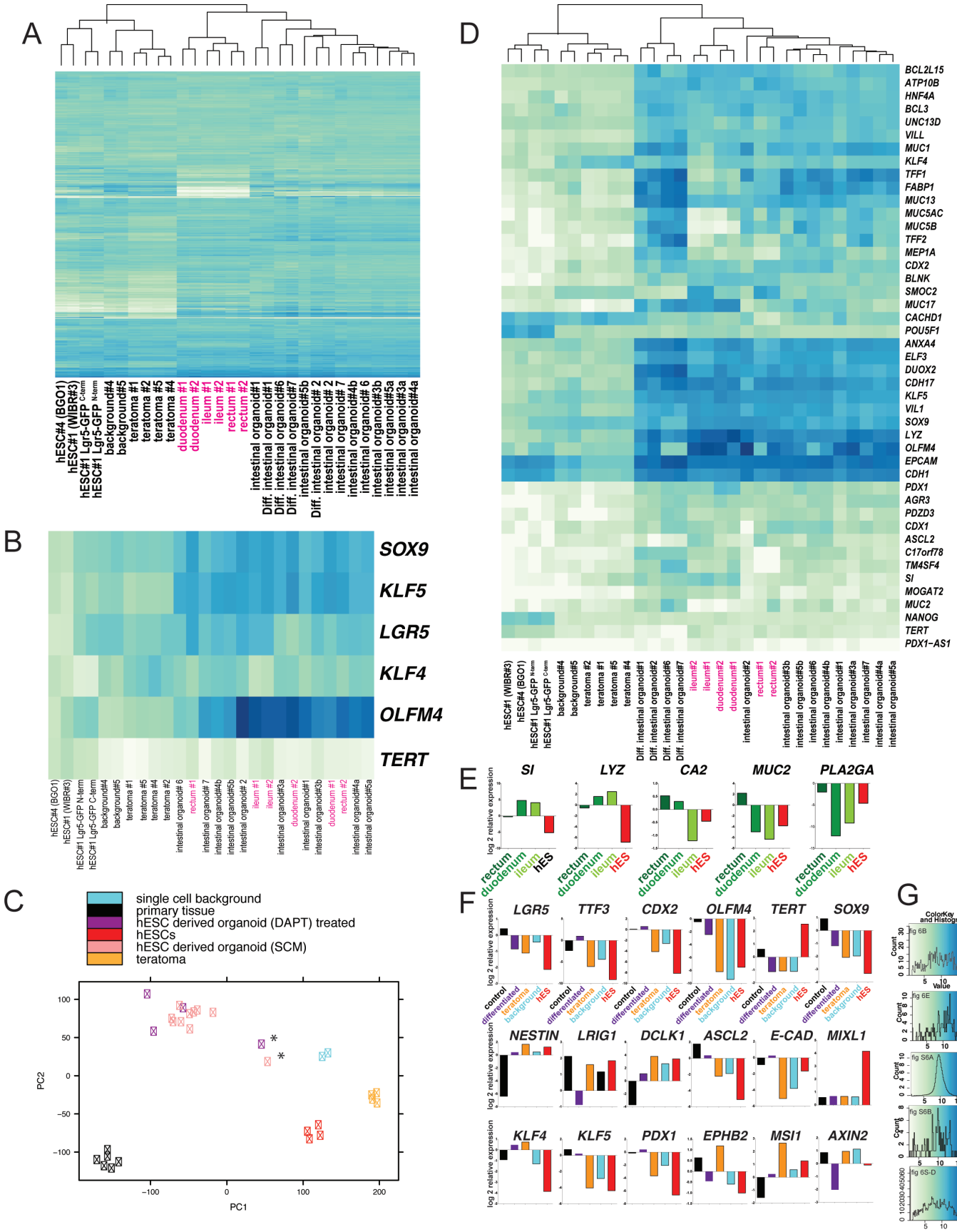
A
hESC#4 (BGO1)
hESC#1 (WIBR#3)
hESC#1 Lgr5-GFP C-term
hESC#1 Lgr5-GFP N-term
background#4
background#5
teratoma #1
teratoma #2
teratoma #5
teratoma #4
duodenum #1
duodenum #2
ileum #1
ileum #2
rectum #1
rectum #2
intestinal organoid#1
Diff. intestinal organoid#1
Diff. intestinal organoid#6
Diff. intestinal organoid#7
intestinal organoid#5b
Diff. intestinal organoid# 2
intestinal organoid# 7
intestinal organoid#4b
intestinal organoid# 6
intestinal organoid#3b
intestinal organoid#5a
intestinal organoid#3a
intestinal organoid#4a
B
SOX9
KLF5
LGR5
KLF4
OLFM4
TERT
C
single cell background
primary tissue
hESC derived organoid (DAPT) treated
hESCs
hESC derived organoid (SCM)
teratoma
PC2
PC1
D
BCL2L15
ATP10B
HNF4A
BCL3
UNC13D
VILL
MUC1
KLF4
TFF1
FABP1
MUC13
MUC5AC
MUC5B
TFF2
MEP1A
CDX2
BLNK
SMOC2
MUC17
CACHD1
POU5F1
ANXA4
ELF3
DUOX2
CDH17
KLF5
VIL1
SOX9
LYZ
OLFM4
EPCAM
CDH1
PDX1
AGR3
PDZD3
CDX1
ASCL2
C17orf78
TM4SF4
SI
MOGAT2
MUC2
NANOG
TERT
PDX1-AS1
E
SI
LYZ
CA2
MUC2
PLA2GA
log 2 relative expression
rectum
duodenum
ileum
hES
F
LGR5
TTF3
CDX2
OLFM4
TERT
SOX9
NESTIN
LRIG1
DCLK1
ASCL2
E-CAD
MIXL1
KLF4
KLF5
PDX1
EPHB2
MSI1
AXIN2
log 2 relative expression
control
differentiated
teratoma
background
hES
G
ColorKey and Histogram
Count
Value
fig 6B
fig 6E
fig S6A
fig S6B
fig 6S-D

Supplemental Table 1

Sample	Tissue	Genetic Background	Group	Growth Cond.
duodenum #1	primary organoid	wt human biopsy	NA	*WENR+ inhibitors
duodenum #2	primary organoid	wt human biopsy	NA	*WENR+ inhibitors
ileum #1	primary organoid	wt human biopsy	NA	*WENR+ inhibitors
ileum #2	primary organoid	wt human biopsy	NA	*WENR+ inhibitors
rectum #1	primary organoid	wt human biopsy	NA	*WENR+ inhibitors
rectum #2	primary organoid	wt human biopsy	NA	*WENR+ inhibitors
intestinal organoid#1	hESC-Organoid	WIBR3- N-term	1	GF-Media
Diff. intestinal organoid#1	hESC-Organoid	WIBR3- N-term	1	**GF -Media+DAPT
hESC#1 LGR5-GFP N-term	hES	WIBR3- N-term	1	hES MEDIA
intestinal organoid# 2	hESC-Organoid	WIBR3- C-term	2	GF-Media
Diff. intestinal organoid# 2	hESC-Organoid	WIBR3- C-term	2	**GF -Media+DAPT
hESC#1 LGR5-GFP C-term	hES	WIBR3- C-term	2	hES MEDIA
hESC#1 (WIBR#3)	hES	WIBR3	3	hES MEDIA
intestinal organoid#3a	hESC-Organoid	WIBR3	3a	GF-Media
teratoma #4	Teratoma	WIBR3-AI9	4	Mouse
intestinal organoid#4a	hESC-Organoid	WIBR3-AI9	4a	GF-Media
teratoma #5	Teratoma	WIBR3-AI9	5	Mouse
intestinal organoid#5a	hESC-Organoid	WIBR3-AI9	5a	GF-Media
teratoma #1	Teratoma	WIBR3	1	Mouse
teratoma #2	Teratoma	WIBR3	2	Mouse
intestinal organoid#3b	hESC-Organoid	WIBR3	3b	GF-Media
intestinal organoid#4b	hESC-Organoid	WIBR3-AI9	4b	GF-Media
intestinal organoid#5b	hESC-Organoid	WIBR3-AI9	5b	GF-Media
intestinal organoid# 6	hESC-Organoid	BGO1	6	GF-Media
Diff. intestinal organoid#6	hESC-Organoid	BGO1	6	**GF -Media+DAPT
intestinal organoid# 7	hESC-Organoid	BGO1	7	GF-Media
Diff. intestinal organoid#7	hESC-Organoid	BGO1	7	*GF -Media+DAPT
background#4	Non-Organoid	WIBR3-AI9	4	GF-Media
background#5	Non-Organoid	WIBR3-AI9	5	GF-Media
hESC#6-7 (BGO1)	hES	BGO1	6,7	hES MEDIA

Footnotes: RNA samples that were analyzed by RNA-seq (column 1). The second column (tissue) indicates the tissue type of each RNA sample. RNA from primary organoid samples was isolated from organoid lines that were cultured for 1-6 months and derived from duodenum, ileum, or rectum biopsies of human subjects.
hESC-derived organoids, hESC and teratoma indicates RNA samples that were isolated from these steps in the differentiation protocol. Non-organoid material indicates single-cell contaminants that were removed by the enrichment protocol described as “single cell background” in the text. The third column indicates the “*Genetic Background*” of the samples in respect to the parent tissue. hESC-derived organoids were isolated from 5 genetically distinct hESC lines: WIBR3, WIBR3 Lgr5-GFP $^{N\text{-}term}$, WIBR3 Lgr5-GFP $^{C\text{-}term}$, WIBR3-AI9, and BGO1. Column 4 shows the correspondence of independently derived teratomas (1-7) to the parental hESCs and derived organoid samples and shows biological replicates (indicated a or b).
The last column shows the specific growth conditions as described in the methods section with GF equivalent to the stem cell growth factors except when differentiation required WNT3a withdrawal. Media called *WENR+inhibitors elsewhere was prepared as described previously (Sato et al., 2011).
**GF-Media+DAPT was GF-Media supplemented with 10μM DAPT and absent Wnt3a for five days.

Supplemental Figure 1: Genome editing of LGR5 locus in WIBR3 hESCs, Teratoma histology and organoid formation

(A) Validating genome-editing activity of engineered ZFNs targeting LGR5 (LGR5 $^{N\text{-term}}$ and LGR5 $^{C\text{-term}}$) in K562 cells. Following transient transfection of the ZFN expression construct, the sequence of the LGR5 locus surrounding the respective ZFN cut sites was PCR-amplified, and genome editing efficiency was measured using the Surveyor nuclease assay. The degree of target locus disruption was quantified and is shown below the lane.

(B) Southern blot analysis of WIBR3 hESCs targeted in the LGR5 locus with the respective donor plasmid shown in Figure 1A. Genomic DNA was digested with HindIII for LGR5-GFP $^{N\text{-term}}$ targeted cells and with EcoRV for LGR5-GFP $^{C\text{-term}}$ targeted cells. DNA was hybridized with the ^{32}P-labeled external 3'-probe or with the internal eGFP probe.

(C) Immunohistochemical staining for indicated proteins in teratoma sections generated from LGR5-GFP $^{N\text{-term}}$ hESC reporter cells (GFP= enhanced green fluorescent protein, large panel shows whole teratoma section with regions of interest showing GFP positive cells in intestinal regions (I-III and V) or other cell types where interpretable [IV: not specified (NS), VI: NS, VII: cartilage, VIII: NS, IX: NS, X: ectoderm/neuroepithelium, XI: neural rosettes].

(D) Immunohistochemical staining for MUC2= mucin2, VIL1= villin1, and CHGA= Chromogranin A in the context of lower magnification images of teratoma sections.

(E) Higher magnification images of independently derived organoids (n=5) on the third day after embedding single-cell dissociated teratoma samples into matrigel. Image shows representative pictures of organoids that form a central lumen at day three.

Supplemental Figure 2: Isolation of intestinal organoids independent of the LGR5-GFP reporter system

(A) Expression profiling of organoids from GFP positive and unsorted LGR5-GFP teratoma cells compared to hESCs and fibroblast-like cells. Quantitative RT-PCR for the indicated genes in hESCs, organoids derived from eGFP-positive cells (n=3) or nonsorted (n=3) cells of LGR5-GFP $^{N\text{-term}}$, hESCs and fibroblast-like cells [derived from hESCs, as described previously (Hockemeyer et al., 2008), expressing telomerase from the AAVS1 locus]. Relative expression levels were normalized to expression levels of these genes in hESCs. Data are biological replicates from independent experiments, bars represent the SEM.

(B) Left: Representative FACS analysis (top) and sorting statistics of LGR5-GFP $^{N\text{-term}}$ hESCs isolated from teratoma explants. Gates were chosen based on undifferentiated hESC cells. Right: Representative FACS analysis (top) and sorting statistics of LGR5-GFP $^{N\text{-term}}$ hESCs isolated from teratoma explants not sorted for GFP, but cultured for 5 days prior to this analysis in organoid culture conditions. FACS settings were identical in both plots.

Supplemental Figure 3: hESC-derived organoids contain Lysozyme positive cells indicating the presence of Paneth cells.

Immunofluorescence staining of a hESC-derived human intestinal organoid stained for Lysozyme (green) and DAPI (red) by confocal microscopy (see also Supplemental movie 1).

Supplemental Figure 4: hESCs and iPSCs can form intestinal organoid cultures when differentiated into a teratoma but not when directly embedded into matrigel.

(A) Left- Undifferentiated hESCs after 5 days grown under intestinal stem cell conditions and embedded into matrigel. Middle panel and right panel show teratoma cells isolated from hESCs and iPSCs after 5 days– grown in parallel under identical conditions.

(B) Increasing magnification top to bottom shows LGR5-GFP N- and C- term derived teratoma cells assayed for the ability to form organoids. Conditions were adapted as described by

(Spence et al., 2011). Cells labeled “Induced” ENR were cultured for 4 days in 500ng/ml FGF4 and 500ng/ml WNT3a (as described in (Spence et al., 2011) and then continuously cultured in ENR. Cells labeled ENR and WENR were cultures as described in methods; ENR/CHIR/NAC as described by (Wang et al., 2013); or WENR + inhibitors as described by (Sato et al., 2011).

(C) A fraction of organoids in “WENR + inhibitors” media showed morphological changes not observed in other conditions, but did not explicitly bud into crypt-like structures after >30 days in culture.

(D) Long-term cultures (>100 days shown) of organoids grown in WENR (not shown) or ENR persist and exhibit increasingly uniform morphology over time.

Supplemental Figure 5: hESC-derived organoids share a transcriptional profile with primary intestinal tissue derived organoids and display the characteristic responses to differentiation stimuli

(A) Heat map of hESCs (n=4), teratoma samples (n=4), bulk hESC-derived organoid cultures grown in WENR (n=10), bulk cultures of hESC-derived organoids grown in differentiation medium (n=4), and primary- duodenum (n=2), rectum (n=2) or ileum (n=2) derived organoids. Shown are the Euclidian distances calculated from the expression of the top 5000 differentially expressed transcripts.

(B) Heat map as in S5A showing selected intestinal stem cell marker genes.

(C) First two components of principal component analysis of expression data from all samples, labeled by sample type. Samples indicated with * were contaminated with non-organoid teratoma cells “single cell background cells” (organoids #1 and organoids #1-differentiated). Early analysis of sample #1 showed unexpected expression; however, subsequent organoids were cultured more stringently as described in methods. “Single cell background” is the RNA isolated from the non-organoid teratoma cells that can be removed partially (please see Supplemental methods and additional discussion of the RNA-seq data) but might represent some residual contamination.

(D) Heat map displaying unbiased cluster analysis of the samples analyzed in Figure 6B, but for an extended subset of genes with intestine specific expression and function. Shown are the Euclidian distances calculated from the relative expression of the genes as determined by RNA-seq.

(E) Intermediate DESeq calculation of RNA-seq results. Shown is the log2 fold change of three types of human-derived intestinal samples and parental hESCs relative to organoids cultured in WENR media (please see supplemental methods).

(F) Intermediate DESeq calculation of RNA-seq results. Shown is the log2 fold change of intestinal stem cell marker genes shown in Figures 2 and S2 for control (all human primary derived samples), differentiated (ENR+DAPT), parental hES, teratoma, and the background (non-organoid cells removed from the cultures) relative to organoids cultured in WENR.

(G) Histograms for heat maps generated for Figures 6B, 6E, S5A, S5B, and S5D.

Supplemental Table 2: RNA-seq Data

Fragments Per Kilobase of transcript per Million mapped reads (FPKM) values for all RNA-seq samples generated as described in materials and methods. The data discussed in this publication have been deposited in NCBI's Gene Expression Omnibus (Edgar, Domrachev, & Lash, 2002) and are accessible through GEO Series accession number GSE56930
http://www.ncbi.nlm.nih.gov/geo/query/acc.cgi?acc=GSE56930

Supplemental Movie1: hESC-derived organoids contain lysozyme positive cells indicating the presence of Paneth cells

Movie of sequential Z-stack of a hESC-derived human intestinal organoid stained for lysozyme (green) and DAPI (red). Please see S3.

Additional discussion of the transcriptional profiling data:

Single cell contaminants can account largely for the expression differences between the hESC derived organoids and primary tissues samples

We also analyzed the genes that were differentially expressed between the human primary-derived samples and the hESC-derived organoids (Supplemental material). Unexpectedly we found a significant enrichment of genes overexpressed in hESC-derived organoid samples, particularly organoid #1 (please see S5C, organoid #1 is indicated with an asterisks). We hypothesized that this difference in gene expression was the result of small amounts of non-organoid differentiated teratoma cells contaminating the hESC-derived organoids. To test this we separated organoids from these single cells and performed transcriptional profiling of both hESC-derived organoids and these single-cell contaminants ("single cell background") that are normally discarded. Indeed, transcriptional profiling of these contaminating cells showed elevated expression of genes with non-intestinal ontology that can largely explain the transcriptional differences between hPSC-derived organoids and primary tissue cultures. Cultures subsequent to the derivation organoid sample #1 were passaged more stringently against the non-enteric teratoma cells as described in the methods and aligned much closer to the profiles of human-derived samples.

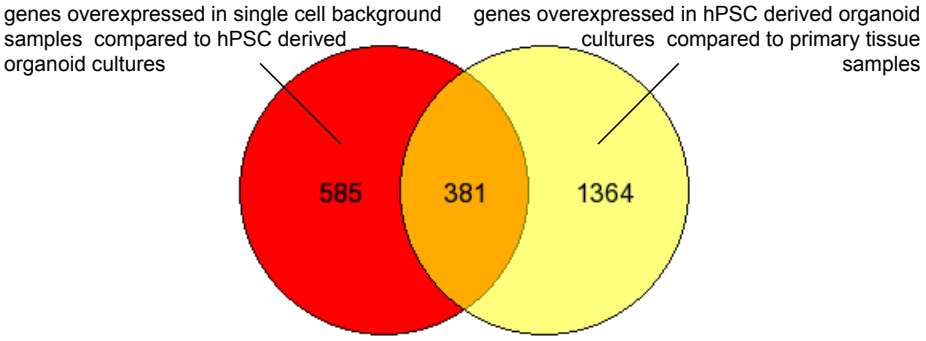

FDR corrected p value for overlap <10-15

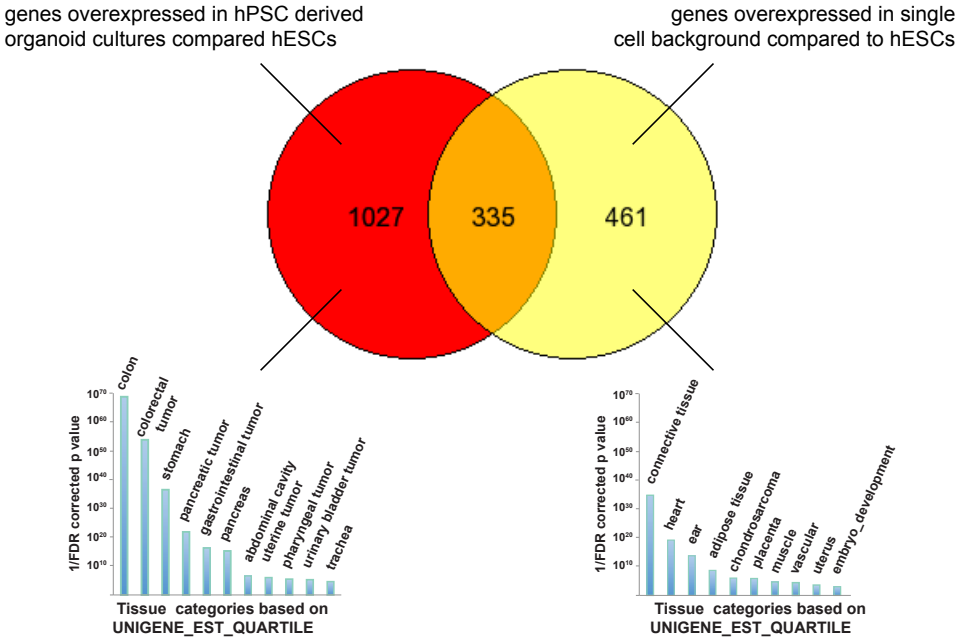

Top: Venn diagram depicting the overlap of genes significantly overexpressed ($p<0.05$ and $2^{2.5}$-fold upregulation) in single cell background samples compared to hPSC-derived organoid cultures and genes overexpressed in hPSC-derived organoid cultures compared to primary tissue samples. Red circle indicates total number of genes overexpressed in background samples (non-organoid outgrowth of teratoma cells) compared to hPSC-derived organoid cultures. Yellow circle indicates total number of genes overexpressed in hPSC-derived organoid cultures compared to primary-derived tissue samples. The high amount of overlap between both gene lists suggests that a significant fraction of the difference between hPSC-derived organoid cultures and primary-derived intestine tissue comes from contamination by background material. P-value for overlap was calculated using a hypergeometric distribution and found to be less than 10^{-15}.

Bottom: Venn diagram depicting the overlap of genes significantly overexpressed ($p<0.05$ and $2^{2.5}$-fold upregulation) in hPSC-derived organoid samples compared to hPSCs as well as genes overexpressed in single-cell background samples compared to hPSC samples. Red circle indicates total number of genes overexpressed hPSC-derived organoid samples compared to hPSCs. Yellow circle indicates total number of genes overexpressed in single-cell background samples compared to hPSC samples. Shown below is the tissue specific expression gene ontology analysis for these genes using the Database for Annotation, Visualization and Integrated Discovery (DAVID; http://david.abcc.ncifcrf.gov/home.jsp) and the “UNIGENE_EST_QUARTILE” expression profile databases. Analyzed were genes significantly (FDR corrected p value <0.05) unregulated (>$2^{2.5}$fold) in hESC-derived intestinal organoids (n=10) compared to hESCs (n=4).

Functional gene ontology analysis of hPSC-derived organoids

Diagrams show the gene ontology using the Gene Ontology enRIchment anaLysis and visuaLizAtion tool (http://cbl-gorilla.cs.technion.ac.il). Genes were ranked by differential expression between hPSC-derived organoids and hESCs. Depicted are biological processes (A), components (B), and functions(C) that are significantly enriched in hPSC-derived organoids.

A

Process:

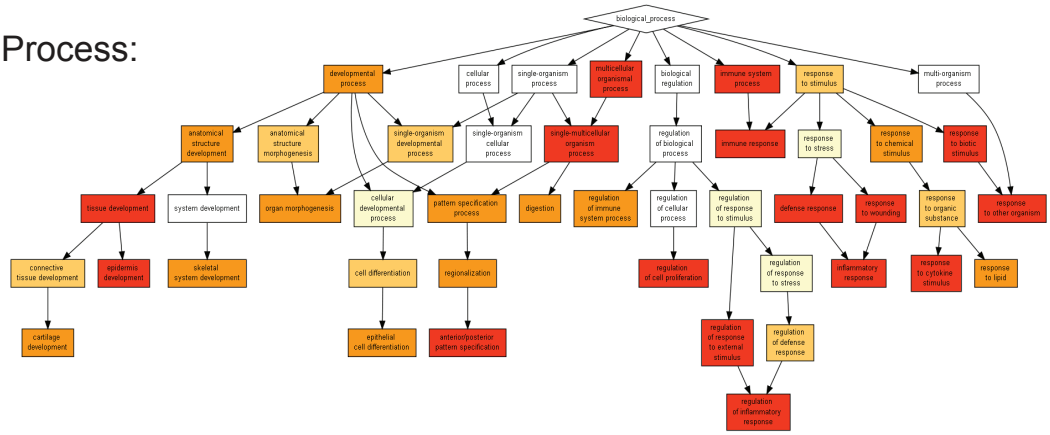

B

Component:

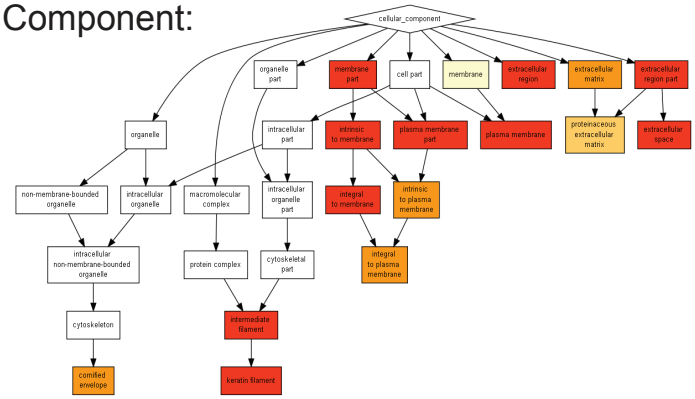

C

Function:

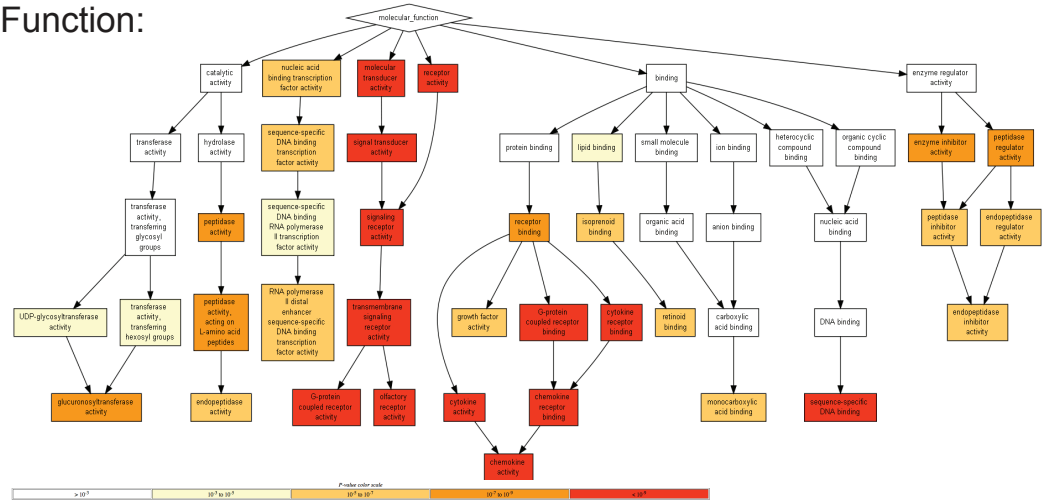

Supplementary Methods

ZFN-driven targeted genetic engineering of the LGR5 locus in hESCs and hiPSCs using ZFN-mediated homologous recombination

hESCs and hiPSCs were cultured in Rho Kinase (ROCK)-inhibitor (Calbiochem; Y-27632) 24 hours prior to electroporation. Cells were harvested using 0.25% trypsin/EDTA solution (Invitrogen), and 1 x 10^7 cells were resuspended in phosphate buffered saline (PBS) and electroporated with 40 µg of donor plasmids (previously described in (Hockemeyer et al., 2009) or designed and assembled by D.H.) and 5 µg of each ZFN or TALEN encoding plasmid (Gene Pulser Xcell System, Bio-Rad: 250 V, 500µ F, 0.4 cm cuvettes). Cells were subsequently plated on MEF feeder layers (DR4 MEFs for puromycin selection) in hESC medium supplemented with ROCK-inhibitor for the first 24 hours. Individual colonies were picked and expanded after puromycin selection (0.5 µg/ml) 10 to 14 days after electroporation. hESC-derived fibroblast-like cells used as negative controls for the expression analysis shown in Figure 2 and Supplemental Figure 2 were generated from hESCs overexpressing hTERT from the AAVS1 locus (unpublished data) by differentiation as previously described in (Hockemeyer et al., 2008).

ZFN design and ZFN expression plasmids

ZFNs against the human LGR5 locus were designed using an archive of validated two- finger modules (Perez et al., 2008; Urnov et al., 2005); complete sequences of the ZFNs, which carried obligate heterodimer forms of the FokI endonuclease (Miller et al., 2007).

ZFN target sites

ZFN Target site and corresponding recognition alpha helices (NH2 to COOH) engineered against the LGR5 locus were as follows: N-term L ZFN target– AATGACAGTGTGTGGGGC, DRSHLTR, RSDHLTT, RSDSLLR, LQHHLTD, DRSNLSR, LRQNLIM; N-term R ZFN target– CCGACGGCAGGAtGTTGCT, QSSDLSR, YKWTLRN, QSGHLAR, QSGDLTR, RSDTLSQ, RSDDRKK; C-term L ZFN target –ACAGTTTAATGGGGG, RSAHLSR, RSDHLST, QSANRTK, TSGSLSR, QSSVRNS; C-term R ZFN target– GGGGTCATCGCAGCAGTG, RSDSLSV, QSGDLTR, QSGDLTR, DTGARLK, DRSALSR, RSDHLSR. The ZFNs were tested by transient transfection into K562 cells followed by Surveyor (Cel-1) endonuclease based measurement of NHEJ at the target locus exactly as described (Miller et al., 2007; Perez et al., 2008).

hESC culture

Cell culture was carried out as described previously (Soldner et all 2009). All hESC lines were maintained on a layer inactivated mouse embryonic fibroblasts (MEFs) in hESC medium (DMEM/F12 [Invitrogen] supplemented with 15% fetal bovine serum [Hyclone], 5% KnockOutTM Serum Replacement [Invitrogen], 1mM glutamine [Invitrogen], 1% nonessential amino acids [Invitrogen], 0.1 mM β-mercaptoethanol [Sigma], penicillin/streptomycin [Gibco], and 4 ng/ml FGF2 [R&D systems]). Cultures were passaged every 5-7 days either manually or enzymatically with collagenase typeIV (Invitrogen; 1.5 mg/ml).

Teratoma Isolation

Subcutaneous hESC-derived teratomas were excised from NOD-SCID mice (Taconic) after 4-8 weeks, briefly washed in 70% EtOH, then PBS supplemented with penicillin/streptomycin. Tissues were minced and disaggregated in 10ml trypsin for 10-15 minutes, treated with 750,000U DNaseI (Roche), and suspended in 30ml of FBS-containing hES media followed by isolation of single cells through a 70μm nylon mesh filter (Falcon) for subsequent FACS or direct matrigel embedding for 3D cultures.

Organoid Reagents and Growth Factors

Matrigel (BD Biosciences), Dispase (Stemcell Technologies),, JAG-1 (AnaSpec; no. 61298), N2 (R&D Systems), B27 (Invitrogen), L-glutamine, NEAA (Gibco), WNT3A (R&D Systems), RSPO1 (R&D Systems), EGF (R&D Systems), Noggin (R&D Systems) and 10μM ROCK inhibitor (Stemgent; Stemolecule™ Y27632)

Immunocytochemistry

Immunostaining of paraffin section was performed with standard techniques using the following antibodies: anti-GFP (Abcam 290), Sox9 (AB5535 Millipore), Mucin2 (H-300 Santa Cruz), Villin (C-19, sc-7672 Santa Cruz), chromogranin A (SP-1 ImmunoStar), EphB2 (AF467 R&D System), Epcam AF960 R&D systems, FABP1 (HPA028275 Sigma), E-cadherin 610181 BD), Lysozyme (Dako), CDX2 (CDX2-88 BioGenex), PDX1 (abcam® ab47267) and appropriate Molecular Probes Alexa Fluor® dye conjugated secondary antibodies (Invitrogen). Phalloidin was Alexa Fluor® 488 Phalloidin or Rhodamine Phalloidin (Molecular Probes – Life Technologies).

Electron microscopy analysis

The material was fixed in 2.5% gluteraldehyde, 3% paraformaldehyde with 5% sucrose in 0.1M sodium cacodylate buffer (pH 7.4). When possible, the organoids were pelleted. Larger organoids

were carried through processing in mesh bottom baskets. Material was post-fixed in 1% OsO4 in veronal-acetate buffer, stained en bloc overnight with 0.5% uranyl acetate in veronal-acetate buffer, dehydrated and embedded in Embed-812 resin. Ultra-thin sections were cut on a Reichert Ultracut E microtome with a Diatome diamond knife, stained with uranyl acetate, and lead citrate. The sections were examined using a FEI Tecnai spirit at 80KV and photographed with an AMT ccd camera.

RT-PCR analysis

RNA was isolated using either the RNeasy Mini Kit (Qiagen) or Trizol extraction followed by ethanol precipitation. Reverse transcription was performed on 150ng of total RNA using oligo dT priming and Thermoscript reverse transcriptase at 50°C (Invitrogen). qRT-PCR was performed in an ABI Prism 7000 (Applied Biosystems) with Platinum SYBR green pPCR SuperMIX-UDG with ROX (Invitrogen) using primers that were in part previously described (Soldner et al., 2009).

qRT-PCR Primer sequences
SOX9F CTGAGCAGCGACGTCATCTC
SOX9R GTTGGGCGGCAGGTACTG
KLF4F ACCAGGCACTACCGTAAACACA
KLF4R GGTCCGACCTGGAAAATGCT
KLF5F CCCTTGCACATACACAATGC
KLF5R GGATGGAGGTGGGGTTAAAT
EOMESF AAGGCATGGGAGGGTATTAT
EOMESR AAACACCACCAAGTCCATCT
VillinF ACACAGGTGGAGGTGCAGAAT
VillinR GGTTGGTCGCTGTCCACTTC
TTF3F CTTGCTGTCCTCCAGCTCT
TTF3R CCGGTTGTTGCACTCCTT
FOXF1F CACTCCCTGGAGCAGCCGTAT C
FOXF1R AAG GCTTGATGTCTTGGTAGGTGA
CDX1F AGCCGTTACATCACAATC
CDX1R GAGACTCGGACCAGACCT
CDX2 B F GAGCTGGAGAAGGAGTTT
CDX2 B R GGTGACGGTGGGGTTTAG
MUC2F TGGGTGTCCTCGTCTCCTACA
MUC2R TGTTGCCAAACCGGTGGTA
ALPF GCAACCCTGCAACCCACCCAAGGAG

ALPR CCAGCATCCAGATGTCCCGGGAG
Sucrase (SI) F TGGCAAGAAAGAAATTTAGTGGA
Sucrase (SI) R TTATTCTCACATTGACAGGATC
Defensin-5 F GACAACCAGGACCTTGCTATCT
Defensin-5 R ACGGGTAGCACAACGGC
Defensin-6F GACAACCAGGACCTTGCTATCT
Defensin-6R ACGGGTAGCACAACGGC

Telomeric repeat amplification protocol (TRAP)

Organoids were isolated from matrigel using dispase, washed with PBS and lysed with HLB buffer (20mM HEPES, 2mM MgCl2, 0.2mM EGTA) and 10% glycerol supplemented with 0.5% CHAPS, 1mM DTT and 0.1mM PMSF. The lysate was rocked at 4° C for 30min and cellular debris was removed by centrifugation. Dilution of the supernatant (0.04 to 1µg of total protein) was incubated with 0.1µg of the TS primer (AATCCGTCGAGCAGAGTT) for primer elongation in TRAP PCR buffer (20mM Tris-HCl pH8.0, 2.5mM $MgCl_2$, 68mM KCl, 0.05% Tween20, 1mM EGTA) including 1mM dNTPs at 30 C° for 1hr. The following PCR reaction was performed supplied with PCR master mix including 0.04µg of the reverse ACX primer (GCGCGGCTTACCCTTACCCTAACC), [α-^{32}P]dGTP (3000 Ci/mmol; PerkinElmer), 1.25 unit of Taq DNA polymerase and 0.04µg of semi-competitive primer sets [TSNT forward primer; ATTCCGTCGAGCAGAGTTAAAAGGCCGAGAAGCGAT, NT reverse primer; ATCGCTTCTCGGCCTTTT) as previously reported (Kim and Wu, 1997)]. The PCR products were analyzed by non-denatured polyacrylamide gel electrophoresis.

Transcriptional profiling

RNA-seq library was prepared at the Functional Genomics Laboratory at UC Berkeley following the standard Illumina library preparation protocol. Total RNA isolation was performed on a pooled culture of organoids from a single 50µl matrigel matrix in the respective condition, colonies of hES cells, or a triturated pellet of minced teratoma. cDNA libraries for high throughput sequencing were prepared from 50~100ng of total RNA from each sample. Ribosomal RNAs were depleted using a oligo(dT) 25 magnetic bead kit (Life Technologies), and the libraries were generated using the PrepX™ SPIA® RNA-Seq and PrepX Library kit (IntegenX) according to the manufacturer's protocol. Then, samples were quantified using the Qubit and PCR amplified for 18 cycles to incorporate indexes and flow cell-binding regions. Final libraries were quantified using the Qubit, Bioanalzyer and qPCR before being sequenced on the HiSeq2000 for 50bps Single-End reads with multiplexing using V3
SBS chemistry reagents.
Reads were mapped to the Ensembl cDNA release 72 (Flicek et al., 2013) with Bowtie2 version 2.1.0

(Langmead and Salzberg, 2012) using the parameters –rdg 6,5, –rfg 6,5, and –score-min L,-.6,-.4. Transcript abundances were calculated with eXpress version 1.4.0 (Roberts and Pachter, 2013) and the resulting effective counts for each transcript were used to calculate fold changes. Effective counts were also processed with DESeq version 1.12.0 (Anders and Huber, 2010) to identify statistically significant differentially expressed genes and transcripts. For bar graphs of gene expression, transcripts were grouped by their originating gene, based on their Ensembl annotation. The expression level of a given gene was calculated as the sum of the estimated abundances of all of its transcripts. The resulting intermediate log2 fold analysis shown as relative expression bar graphs used DESeq normalized expression results to generate pair wise analysis. Experiments were clustered using complete linkage clustering applied to abundance estimates and projection of the transcript abundance matrix onto the first two principal components was used to visualize similarity between experiments. IGV version 2.3.13 (Thorvaldsdóttir et al., 2013) was used to create read coverage tracks. FPKM available in supplement and raw data for RNA-seq is available at http://www.ncbi.nlm.nih.gov/geo/ (GSE56930).

Supplementary References:

Edgar, R., Domrachev, M., & Lash, A. E. (2002). Gene Expression Omnibus: NCBI gene expression and hybridization array data repository. *Nucleic Acids Research*, *30*(1), 207–210.

Hockemeyer, D., Soldner, F., Cook, E.G., Gao, Q., Mitalipova, M., and Jaenisch, R. (2008). A drug-inducible system for direct reprogramming of human somatic cells to pluripotency. Cell stem cell *3*, 346-353.

Miller, J., Holmes, M., Wang, J., Guschin, D., Lee, Y., Rupniewski, I., Beausejour, C., Waite, A., Wang, N., Kim, K.*, et al.* (2007). An improved zinc-finger nuclease architecture for highly specific genome editing. Nature biotechnology *25*, 778-785.

Perez, E., Wang, J., Miller, J., Jouvenot, Y., Kim, K., Liu, O., Wang, N., Lee, G., Bartsevich, V., Lee, Y.*, et al.* (2008). Establishment of HIV-1 resistance in CD4+ T cells by genome editing using zinc-finger nucleases. Nature biotechnology *26*, 808-816.

Sato, T., Stange, D.E., Ferrante, M., Vries, R.G.J., van Es, J.H., van den Brink, S., Van Houdt, W.J., Pronk, A., Van Gorp, J., Siersema, P.D.*, et al.* (2011). Long-term expansion of epithelial organoids from human colon, adenoma, adenocarcinoma, and Barrett's epithelium. Gastroenterology *141*, 1762-1772.

Spence, J.R., Mayhew, C.N., Rankin, S.A., Kuhar, M.F., Vallance, J.E., Tolle, K., Hoskins, E.E., Kalinichenko, V.V., Wells, S.I., Zorn, A.M.*, et al.* (2011). Directed differentiation of human pluripotent stem cells into intestinal tissue in vitro. Nature *470*, 105-109.

Wang, F., Scoville, D., He, X.C., Mahe, M.M., Box, A., Perry, J.M., Smith, N.R., Lei, N.Y., Davies, P.S., Fuller, M.K.*, et al.* (2013). Isolation and characterization of intestinal stem cells based on surface marker combinations and colony-formation assay. Gastroenterology *145*, 383-395 e381-321.